Journal of
Manufacturing and Materials Processing

Review

Sustainable Manufacturability of Archimedes Screw Turbines: A Critical Review

Aristotle T. Ubando [1,2,3,*], Isidro Antonio V. Marfori III [1,4], Marnel S. Peradilla [5], Charlle L. Sy [6], Andre Marvin A. Calapatia [1] and Wei-Hsin Chen [7,8,9]

1 Department of Mechanical Engineering, De La Salle University, 2401 Taft Avenue, Manila 0922, Philippines
2 Thermomechanical Analysis Laboratory, De La Salle University, Laguna Campus, LTI Spine Road, Laguna 4024, Philippines
3 Center for Engineering and Sustainable Development Research, De La Salle University, 2401 Taft Avenue, Manila 0922, Philippines
4 Center for Micro-Hydro Technology for Rural Electrification, De La Salle University, 2401 Taft Avenue, Manila 0922, Philippines
5 Department of Computer Technology, De La Salle University, 2401 Taft Avenue, Manila 0922, Philippines
6 Department of Industrial and Systems Engineering, De La Salle University, 2401 Taft Avenue, Manila 0922, Philippines
7 Department of Aeronautics and Astronautics, National Cheng Kung University, Tainan 701, Taiwan
8 Research Center for Smart Sustainable Circular Economy, Tunghai University, Taichung 407, Taiwan
9 Department of Mechanical Engineering, National Chin-Yi University of Technology, Taichung 411, Taiwan
* Correspondence: aristotle.ubando@dlsu.edu.ph

check for updates

Citation: Ubando, A.T.; Marfori, I.A.V., III; Peradilla, M.S.; Sy, C.L.; Calapatia, A.M.A.; Chen, W.-H. Sustainable Manufacturability of Archimedes Screw Turbines: A Critical Review. *J. Manuf. Mater. Process.* **2022**, *6*, 161. https://doi.org/10.3390/jmmp6060161

Academic Editor: Steven Y. Liang

Received: 17 November 2022
Accepted: 9 December 2022
Published: 13 December 2022

Abstract: Archimedes screw turbines are considered a new technology in small- or microscale hydropower. Archimedes screw turbines are easy and practical to operate. However, their manufacturing presents some challenges owing to their screw-shaped design. Most of the previous works on Archimedes screw turbines focused on the turbines' design, while limited studies were found on their manufacturing processes. In addition, no review work was found on the manufacturability of the Archimedes screw turbine. Hence, this work aims to address this gap by reviewing the various manufacturing methods of Archimedes screw turbines. Moreover, one of the objectives of the study is to assess the sustainable manufacturability of the Archimedes screw turbine. The results show that Archimedes screw turbines are mainly manufactured using conventional manufacturing methods for larger turbines and 3D printers for relatively smaller ones. Traditional methods of manufacturing entailed high skill proficiency, while 3D-printing methods for Archimedes screw turbines are still in their early developmental stages. Sustainable assessment studies have identified additive manufacturing as having a relatively lower environmental impact than conventional manufacturing on turbine blades. These trade-offs must be accounted for in the design and development of Archimedes screw turbines. Moreover, integrating sustainability assessment and the employment of Industry 4.0 enables the smart production and sustainable assessment of AST manufacturability.

Keywords: Archimedes screw turbines; additive manufacturing; hydropower; Industry 4.0; sustainability assessment; manufacturability

1. Introduction

With the continuous rise of global carbon dioxide (CO_2) emissions brought by the production of energy through fossil fuels, a renewable energy source is needed to satisfy the global energy demand while mitigating CO_2 emissions [1]. One of the matured and accepted renewable energy technologies is hydropower [2]. In areas that are off-grid with access to elevated running water, small- and micro-hydropower sources are suitable renewable energy technologies [3]. However, conventional hydropower turbine designs present risks in harming aquatic biodiversity. Hence, a unique turbine design such as the

Archimedes screw turbine (AST) provides a safe solution for generating hydropower for areas with high aquatic biodiversity [4].

The AST is a hydroturbine that is geometrically modeled after Archimedean screws, which are machines historically used to pump water to higher elevations [5]. The Archimedes screw was initially introduced by Archimedes, the Greek Mathematician; its intended use was pumping of water found in ships [6]. In the first century BC, Vitruvius extensively studied the various applications of Archimedean screw pumps [7]. Being modeled after Archimedean screws, ASTs generally have two components, the helical screw blades and the screw shaft [8]. ASTs utilize this function of Archimedean screws inversely to harness hydropower. Flowing water enters the inlet channel of the AST, and as flowing water is continuously carried downstream in "buckets" due to the helical orientation of the screw blades, momentum from the flowing water rotates the screw blades and, consequently, the screw shaft, which is coupled to a generator to produce electrical power. Figure 1 below shows an image of an animated computer-aided design (CAD) model of an AST showing downstream and upstream basins, the helical screw blades, and the screw shaft.

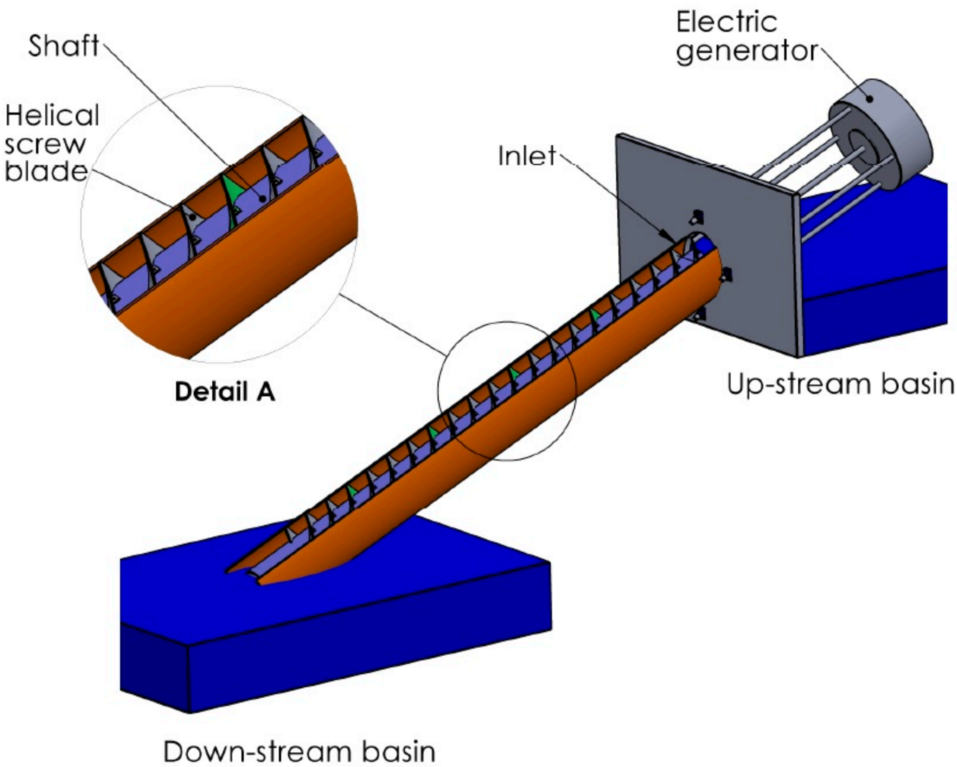

Figure 1. Rendered CAD model of an Archimedes screw turbine.

Using ASTs has several advantages over the usage of conventional hydroturbines. Several studies have claimed that their manufacturing method is simpler than conventional hydroturbines, making them relatively inexpensive and easily manufacturable [9–11]. ASTs ideally operate in low-head conditions and low rotational speeds [12]. This is advantageous in off-grid applications in rural communities with access to running bodies of water since high-elevation water sources are not required and fish passage is undisturbed [13,14]. Fish migration studies have recommended using ASTs to lower mortality and injury rates across multiple species of fish [15–17]. Furthermore, in Europe, a total of 74 hydropower plants operated by ASTs were documented in a 2015 survey, with installed operating capacities varying from 6 kW to 140 kW [5]. The wide utilization of ASTs in the industry shows the potential of ASTs as a sustainable renewable energy technology.

The techniques and methods used to manufacture ASTs must be documented to elucidate the feasibility of manufacturing ASTs in any given region. This will now open opportunities for prospective manufacturers of AST parts that address the installation and logistical concerns. Few review works were found in the Scopus database, ScienceDirect database, and open access journals (4 November 2022) that utilized Archimedes screws as turbines to generate renewable energy. The following works are review studies relevant to the Archimedes screw turbine. Simmons and Lubitz [18] reviewed experimental and numerical studies of Archimedes screw generators and found insufficient verification to be implemented on a commercial scale. Their results also indicated that modern sheet metal manufacturing techniques have made AST manufacturing cost-effective. Waters and Aggidis [5] reviewed the various operational modes of the Archimedes screw from turbines to pumps and have revealed that the computational fluid dynamics (CFD) approach is a viable validation approach for the design and utilization of AST.

In addition, two relevant studies were found in the ScienceDirect database (4 November 2022) that cited that Archimedes screw turbines produce renewable energy. Waters and Aggidis [19] outlined that Archimedes screw turbines, along with other unique turbine designs, can be used for tidal energy conversion, while Hoffstaedt et al. [11] highlighted that rotary positive displacement and counter-rotating reversible turbines and pumps, such as Archimedes screws, are technologies that are used for pumped hydro storage. Furthermore, two brief review works were found in open access journals. Suraya et al. [20] briefly reviewed various studies based on the parameters investigated in the design of the turbine, such as head, screw diameter, pitch diameter, slope angle, the number of rotations, and their effect on turbine efficiency. Meanwhile, Yoosefdoost and Lubitz [4] compared ASTs to other conventional hydroturbines in terms of capital cost, maintenance cost, and environmental and social advantages and presented potential design guidelines for the turbines concerning site evaluation, screw geometry, and generated power output. Lastly, Poosti et al. [21] reviewed the various operational concerns of the different types of Archimedes screw pumps and turbines to further enhance the operation of a commercial wastewater treatment plant. These review works are significant in the advancement of AST for the production of renewable energy. However, these studies did not concentrate on the manufacturing methods of ASTs.

Currently, there is no review work found that focuses on the manufacturability of ASTs. Hence, this review work aims to address this research gap by providing a systematic approach in the review of related literature on the sustainable manufacturing methods of ASTs. In addition, the study also aims to present these methods used for the manufacturing of ASTs and their optimal design parameters.

2. Bibliometric Review on Archimedes Screw Turbines

The goal of the bibliometric review of this study was to identify the whole scope of AST research and identify any works that pertain to the manufacturability of ASTs. The methodological framework of this review can be seen below in Figure 2. The bulk of the research documents used for review was obtained from Scopus and Google Scholar.

In this bibliometric study, statistics of various works and documents made on ASTs were collected, a network map was created to determine the research scope of AST research, and the research gap of manufacturability of AST was analyzed. The scientific database used in this study for collecting document statistics was Scopus Index, and VOSviewer was used to construct the network map.

To identify the whole scope of AST research, a specific search query was carefully constructed to guarantee that a search in Scopus Index would return all results that included AST research. As such, nomenclatures in AST research were initially investigated, and it was found that various research works referred to ASTs differently. Some of the nomenclature used instead of "Archimedes screw turbine" were "Archimedes turbine" [22], "Archimedes generator" [23], "Archimedes screw generator" [9,24,25], and "screw turbine" [26]. Search results from all these names were combined to describe the whole scope of AST research. A total of 109 documents were obtained from the Scopus search results on 4 November 2022. Among these 109 documents, there were 67 articles and 5 reviews.

Further screening of the 109 documents was performed by filtering relevant studies based on the scope of engineering and documents within the ScienceDirect database and open access journals.

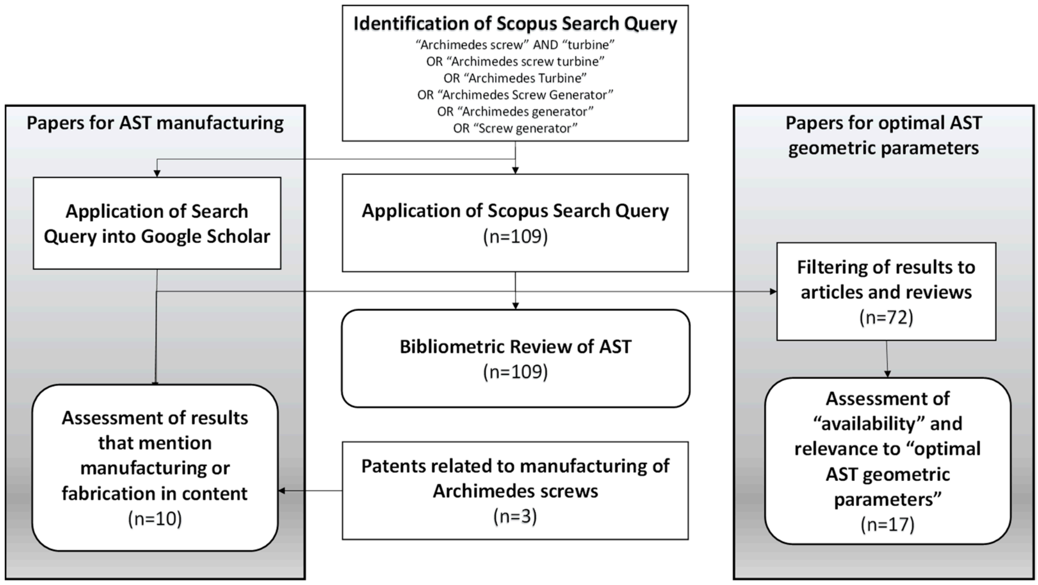

Figure 2. The methodological framework of the systematic review.

After collecting the statistics of the search results, VOSviewer was used to generate the network map of all the search results. The network map contained indexed keywords that commonly occurred among the search results, which is useful in identifying research gaps. An occurrence threshold of 3 was used, given the relatively small result size of the literature scope, and the network map was generated, as seen in Figure 3.

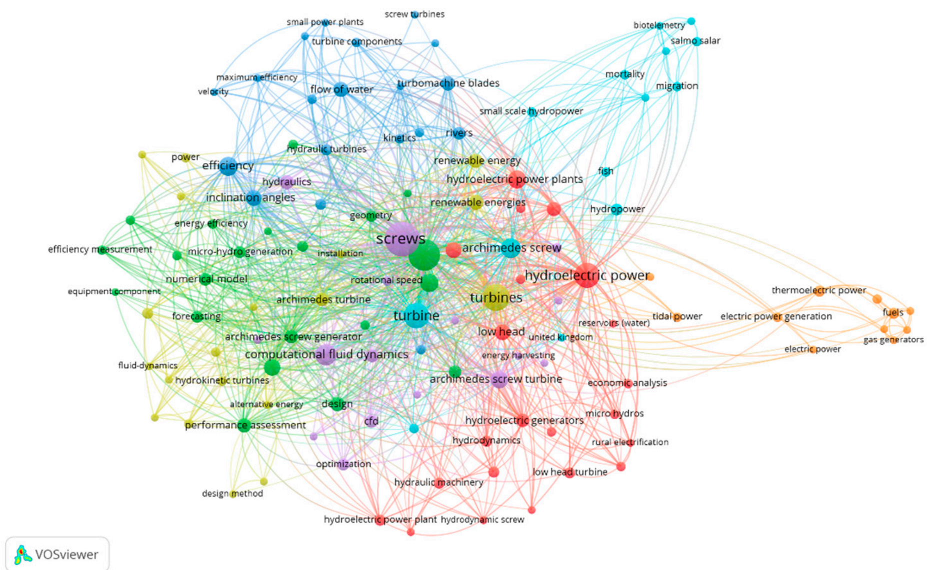

Figure 3. Network map of AST research field from Scopus database.

Major keywords were identified, such as screws, turbine, hydroelectric power, efficiency, and computational fluid dynamics (CFD). These findings indicate that these subjects are currently the main research areas of interest in the scientific community, and most research on ASTs falls under these categories. The results revealed that current AST research shows minimal work on AST manufacturing or production. Most of the recent AST research is focused on hydropower generation, technical design, CFD, and the association of AST with conventional sources of energy. Furthermore, search queries in Scopus combining the keywords of "AST" and "manufacturability" have shown no results, thus indicating that no review works were found.

Using data from Scopus database, yearly publications on AST research were also analyzed. These publications are graphically presented in three-year periods in Figure 4. A total of 109 documents were published in the available literature starting from 1970, and over 95.7% of all those documents were published after 2011. Notably, research interest in AST grew exponentially after 2013, which saw an average of 36 publications every three years, whereas there were only three publications from 2001 to 2012. Considering its low research volume, AST research is not as large as other research fields (e.g., impulse turbine research has 615 results, and Francis turbine research has 2355 results). Furthermore, the first industrial application of ASTs in hydropower plants was not realized until 1994 [5]. Thus, ASTs are still considered an emerging renewable energy technology. ASTs have immense potential for research application and commercialization.

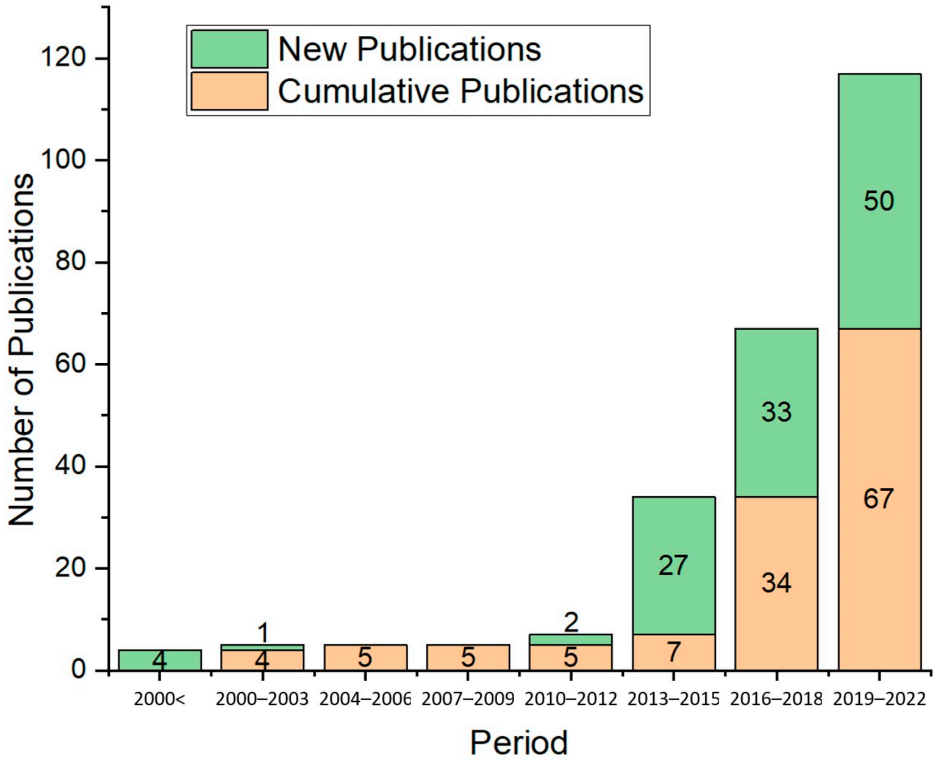

Figure 4. Total publications on AST research since year 2000 in the Scopus database.

3. Optimal Design Parameters of Archimedes Screw Turbines

This section discusses the various research works that investigated different methodologies, tools, and processes to obtain the optimal geometric parameters and operating design conditions that would allow the Archimedes screw turbine (AST) to achieve the highest efficiency. Table 1 shows a summary of the major contributions of each reviewed work on the optimal design parameters of AST, and Table 2 shows a summary of the optimal geometric parameters of each AST.

Table 1. Summary of notable research contributions to optimal design parameters in AST research.

References	Main Contributions
Dellinger et al. [25]	• Showed that the ideal inclination angle varies with the number of blades on the AST, with 15° for 3-blade, 20° for 4-blade, and 25° for 5-blade, with 5-blade generating the most power.
Rorres [7]	• Computed the optimal diameter ratio of 0.54 for AST, which has been referenced by hundreds of works.
Lashofer et al. [27]	• Recommended the diameter ratio of 0.5 for Archimedes screw pumps, which has been referenced by a few works.
Simmons et al. [28]	• Determined the optimal length–pitch ratio of 1.0 for AST. • Showed longer AST screws perform better (L/p > 3.0).
Alonso-Martinez [29]	• Showed that control of rotational speed is essential in efficiency. • Proposed a new methodology in designing efficient AST wherein a filling level of 85% was prescribed by relating the effect of filling factor to efficiency.
Edirisinghe et al. [30]	• Experimental study on AST found optimal screw angle inclination was 22° at a maximum efficiency of 74.27%. • Showed that high inclination angles on AST can also reach 80% efficiency.
Saroinsong et al. [31]	• Analyzed that the fluid phenomena occurring between the screw blades were in the form of vortices, which were experimentally shown to reduce efficiency, but can be mitigated by reducing screw angle inclination. • Optimal values of λ, F_r, and β were $1.0r_o$, 0.12, and 25° at an efficiency of 89%.
Shahverdi [32]	• Used a combined approach of RSM and Buckingham Pi theorem to predict the optimal configurations of an AST. • Optimal values of β, D_o/H, and N were 27°, 0.731, and 4 blades, at an efficiency of 83.4%.
Lee and Lee [33]	• Conducted experimental tests on an AST at high screw angle inclinations (30° to 90°) • Optimal values of β and u were at 45° and 1.5 m/s, at a mechanical efficiency of 94.6%.
Shahverdi et al. [34]	• Developed a numerical model which optimized the geometric parameters of an AST in MATLAB. • Optimal values of L, β, and N were 6 m, 20°, and one blade, at a mechanical efficiency of 90.83%.
Dedić-Jandrek and Nižetić [35]	• AST generally perform better with AC generators than DC generators.
Maulana et al. [36]	• Experimental relationship of flow rate, efficiency, and power output wherein maximal efficiency is found between the extrema or minima of the design flow rate.
Betancour et al. [37]	• Used RSM and statistical analysis to create a characteristics equation that relates diameter ratio, screw length, and screw pitch to power coefficient. • Optimal values for D_i/D_o, L, and p were 0.2, 0.12 m, and 0.30 m.
Bouvant et al. [10]	• Optimal values for D_i/D_o, L, p, and α were 0.1 m, 0.36 m, 0.22 m, and 73.94°.

The geometric parameters of an AST can be seen below in Figure 5 in the form of a schematic diagram. The summary of the nomenclature used in the diagram are as follows: L is for the screw length, P is for the screw pitch, β is for screw angle inclination, α is for screw blade angle inclination, D_o is for outer diameter, D_i is for inner diameter, and the numbers 1 to 5 denote each blade in the design.

Table 2. Summary of the optimal geometric parameters of each AST type (numerical model or experimental prototype.

Reference	Type of Study	L m	P m	N Blades	β °	α °	D_i mm	D_o mm	Q L/s	H m	ω rpm	η %
Dellinger et al. [24]	Numerical	0.40	0.19	3	24.0		104	192	2.8		84.6	77.0
Zitti et al. [38]	Experimental	0.32	0.16		0.0	70.0	20	50			28.6	23.8
Rohmer et al. [39]	Numerical		0.96	3	30.0		420	840	90		40	84.0
Erinofiardi et al. [26]	Experimental				45				0.68	0.05	946	92.0
Abdullah et al. [40]	Experimental	1.0	0.07	1	35		70	130	1.12		165	81.4
Durrani et al. [41]	Numerical		1.71	3	26		640	1200	240	1.5	27.6	77.0
Syam et al. [42]	Experimental	2.0	0.26	1	30		140	260	20	1.0	236.4	57.0
Dellinger et al. [25]	Numerical			5	24.5						50.0	85.8
Thakur et al. [43]	Experimental	1.63	0.30		22.0		80	200	1.0 to 4.0			74.3
Edirisinghe et al. [30]	Numerical	7.78	0.84	3	45.0		1296	2400	200	5.2	54.6	82.1
Saroinsong et al. [31]	Experimental	0.92	0.13	3	25.0	30.0	600	1100			50	89.0
Shahverdi [32]	Numerical			4	27.3		78	156	0.95	0.27	106	83.4
Lee and Lee [33]	Experimental	1.50	0.15	1	45.0		60	120	0.3 to 1.7	1.0	179.8	94.6
Shahverdi et al. [34]	Numerical	6.00	1.50	1	20		750	1500	1200	1.8	91.1	90.8
Dedić-Jandrek and Nižetić [35]	Experimental	1.00	0.30	3	21		160	300	10	0.5	70	67.0
Maulana et al. [36]	Experimental	2.00	0.29	2	30		77	144	12.5	1.0	177	55%
Betancour et al. [37]	Numerical	0.12	0.30									50.6
Bouvant et al. [10]	Numerical	0.36	0.22			73.9						55.2

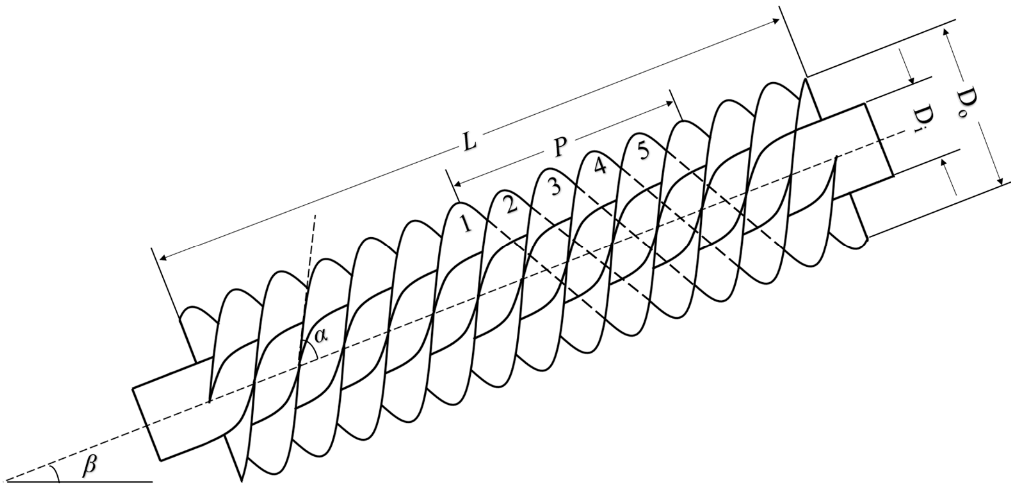

Figure 5. Geometric diagram of a typical Archimedes screw turbine.

One of the most prominent works in AST research is the study conducted by Rorres [7], which defined the AST optimal diameter ratio, the ratio of inner diameter to the outer diameter, to be at a value of 0.54. The idea behind this computed value was to maximize the volume of carried water in the buckets of the AST, although this work is mostly based on an Archimedes pump rather than that of a turbine. Rorres [7] compared the computed values from other Archimedes screws in the literature, namely, screws designed by the Roman engineer, Vitruvius, and the general design of modern Archimedes screws.

Several other works were highlighted by Rorres [7] for the development of the Archimedes screws and are discussed as follows. Dellinger et al. [25] performed an in-depth CFD analysis on Archimedes screw generators and showed that the best slope to have to provide a high efficiency is from 20° to 24.5°. Alonso-Martinez [29] proposed a methodology to design ASTs by targeting an 85% filled bucket level while minimizing system leakage. Edirisinghe et al. [30] conducted a CFD study of an actual site of ASTs with an inclination angle of 45°, which resulted in an efficiency of 82%. Their results have proven that even at a high inclination angle, comparable efficiencies of ASTs can still be achieved in a run-off river [30]. Dedić-Jandrek and Nižetić [35] evaluated an AST hydropower test station and found that a maximum efficiency of 64% is attained at an inclination angle of 21° with a flowrate of 36 $m^3\ h^{-1}$ and a power output of 35 W. Maulana et al. [36] experimentally evaluated a double-bladed AST and revealed a maximum turbine efficiency of 55% at 45 $m^3\ h^{-1}$ and a maximum power output of 116 W at 90 $m^3\ h^{-1}$. Bouvant et al. [10] performed a CFD study coupled with the response surface method to optimize the geometric parameters of an AST under six degrees of freedom. Their results revealed that the optimal configuration of ASTs has dimensions such as a diameter ratio of 0.1, length of 0.36 m, an inclination angle of about 74°, and a blade stride of 0.22 m [10]. Simmons and Lubitz [44] also employed CFD to analyze the behavior of fluid flow inside the buckets of the AST and was accurately validated by experimental laboratory-scale data. Lastly, Lashofer et al. [45] and Lashofer et al. [27] recommended that the diameter ratio for Archimedes screws be at 0.5 for pump applications. These studies highlighted the influence of parametric design on the performance of ASTs through CFD. CFD is a numerical method to design ASTs through parametric dimensional factors and assess fluid flow behavior and power performance [40,46].

To further understand the progress on the optimal design of ASTs, the following studies are discussed in detail. Simmons et al. [9] conducted surveys and measurements on various AST powerplants in the United Kingdom, measuring geometric parameters and flowrate data. Their study also evaluated the optimal geometric parameters of an AST in terms of inclination angle, pitch–diameter ratio, pitch–length ratio, and the number of blades [9]. Meanwhile, Dellinger et al. [25] investigated the effects of the screw angle inclination (β) and the blade number (N) on the power output and efficiency. Their results obtained an optimal inclination angle of 22°, which agreed with the optimal angle that other studies found, i.e., in the range of 20° to 25°. However, Dellinger et al. [25] emphasized that the optimal angle depends on the site constraint where the hydro powerplant is situated. Three numerical models with different blade numbers (i.e., 3, 4, and 5 blades) were numerically modeled in OpenFOAM, with the fluid domain being constructed in blockMesh and the screw rotation realized using the Arbitrary Mesh Interface method. All simulations were run at 50 rpm and with flow rates varying from 28.8 $m^3\ h^{-1}$, 30.6 $m^3\ h^{-1}$, and 32.4 $m^3\ h^{-1}$. Experimental runs were conducted using an existing prototype to compare the experimental results with the CFD results, and good agreement was found in their comparison. For each type of AST in the numerical simulation, the β values tested were 10°, 15.5°, 20°, 24.5°, 29°, 33.5°, and 38°. Results show that for a three-blade, four-blade, and five-blade AST, the optimal values of β were found at 15.5°, 20°, and 24.5°, and the corresponding power outputs and efficiencies at these β values were 25.7 W and 86.1%, 34.1 W and 86.3%, and 37.3 W and 85.8%, respectively. The most optimal blade configuration, in this case, was found to be that with 5 blades and an inclination of 24.5°.

In their other study, Simmons et al. [28] investigated three different pitch–diameter ratios (0.8, 1.0, and 1.4) and three ranges of length–pitch ratios with laboratory-scale experimentation (<1.5, 1.5 to 3.0, >3.0). Their results showed that the AST with a pitch–diameter ratio of 1.0 performed the most efficiently. Moreover, the results outlined that the AST with a relatively higher length–pitch ratio performed better compared to those that have relatively lower length–pitch ratios. Simmons et al. [28] further theorized that the AST has more time to fully form its water buckets and convert hydrodynamic forces into torque when the screw is longer. However, the mechanical advantages are offset by the increased manufacturing costs, heavier system loads, and larger losses from friction.

Alonso-Martinez [29] developed a new methodology for designing ASTs that served to further increase their resulting efficiency. When an AST experiences leakage losses, the resulting torque decreases, and, consequentially, its efficiency decreases as well. Thus, a hypothesis was constructed to quantify leakage losses, and it described a linear relationship between the leakage losses and rotational speed, as shown in Equation (1).

$$\frac{Q_{leak}}{Q_{max}} = L_s + L_s \frac{\omega}{60} \frac{Q}{Q_{max}} \quad (1)$$

where Q_{leak} is leakage loss (m^3 s^{-1}), Q_{max} is the maximum design flowrate (m^3 s^{-1}), ω is rotational speed (rpm), and Q is the design flowrate (m^3 s^{-1}).

Their hypothesis was compared with the efficiency curves of other works and was used to establish two significant design considerations for high-efficiency AST. The first design consideration of the AST must be viewed as a bucket elevator and must have a filling level considered in its designs. The second design consideration of the AST includes minimizing the leakage loss to as low a level as possible. Alonso-Martinez [29] developed four numerical models of the AST using the finite element method to understand the relationship of the filling level (Q/Q_{max}) with the torque at different filling levels (i.e., 41%, 52%, 69%, and 85%). A small-scale and real-scale prototype was manufactured to analyze the effects of real-world leakage losses on AST performance. Based on the proposed methodology to minimize leakage losses, the small-scale prototype was manufactured to analyze its efficiency under different flow conditions. The real-scale prototype was manufactured under the same methodology but was integrated with variable speed control. The numerical results showed that the torque was directly proportional to the filling level of the buckets, with an R2 of 1.0. The torques were 10 N-m, 13 N-m, 17 N-m, and 21 N-m at the filling levels of 41%, 52%, 69%, and 85%, respectively. Thus, based on the hypothesis and these numerical results, it was verified that the rotational speed affects the efficiency. The small-scale prototype experiments showed the system operated near 90% efficiency when the filling level was more than 85%, and leakage losses increased linearly with the filling factor, which verified the hypothesis of the study. The real-scale prototype experiments operated near 85% efficiency when the filling level was more than 60%. The leakage losses in the small-scale and real-scale prototypes ranged from 5% to 10% and 6% to 9%, respectively. The study concluded that a filling level of 85% was ideal since operating conditions with filling levels above 85% were prone to overflowing. Additionally, active speed control was prescribed to control the rotational speed of the AST.

Thakur et al. [43] conducted a simple experimental study using an AST prototype to maximize its efficiency. The prototype used had the following geometric parameters: screw length (L) was 1.63 m, inner diameter (D_i) was 0.08 m, outer diameter (D_o) was 0.2 m, and pitch (P) was 0.3 m. The flow rate (Q) was altered between 3.6 m^3 h^{-1} to 14.4 m^3 h^{-1}, the screw angle inclination changed between 20° to 25°, and the load varied at 0.5 kg, 0.7 kg, and 0.9 kg. From the experimental results, the load was shown to have a directly proportional relationship with efficiency, although the efficiency was lowest at the highest flow rate with a parabolic trend, and the maximal efficiency of 74.27% was at 22° while showing a nonlinear relationship.

Edirisinghe et al. [30] stressed that most works on AST focused on maximizing efficiencies, commonly more than 80%, on small inclination angles, but such small inclination angles pose high bending loads when installed onsite due to the long screw length of the AST. Consequentially, Edirisinghe et al. [30] investigated the potential of high screw inclination angles to achieve the near-same values of efficiency that AST would have with low-angle configurations. The site considered for the CFD simulation had a head (H) of 5.2 m and an average flow rate (Q) of 0.23 m^3 s^{-1}. The design procedure of the screw mostly referenced Rorres' work on optimum geometric ratios of ASTs. For a screw angle inclination (β) of 45°, the diameter ratio was 0.54, the screw pitch (P) was 0.84 m, and the screw length (L) was 7.78 m for the three-bladed AST. The numerical model was constructed in SOLIDWORKS 2016 and was meshed and solved in ANSYS ICEM CFD 19.2. Numerical simulations were run at different rotational speeds (ω) of 40 rpm, 50 rpm, 54 rpm, 58 rpm, 60 rpm, and 70 rpm. They validated the CFD results with a similar work from the literature. Results were validated with a reference study, and they showed that at the optimal rotational speed of 54.58 rpm, the output power was 9.7 kW and the maximum efficiency was 82.1%. This research was able to show that high inclination angles of ASTs are feasible alternatives in the scenario in which the hydraulic head is too high, which would otherwise cause a low-angle AST to have very long design screw lengths and cause it to bear high bending loads.

Saroinsong et al. [31] experimentally investigated the fluid flow phenomena at the turbine screw of an AST. They stated that since the main driving force of an AST is the gravitational force, the Froude number (Fr) was an important metric used in the study; thus, they wanted to see the effects of Fr on efficiency. The fluid flow phenomena were physically observed using an existing AST prototype with three blades, a screw blade angle (α) of 30°, a diameter ratio of 0.54, and a pitch of 0.132 m. For the experiment, Fr was varied using three of its parameters: screw angle inclination (β), characteristic length (λ), and inflow velocity (u), which had value ranges based on the AST outer radius (r_o) from 25° to 45°, $0.5r_o$ to $1.0r_o$, and 0.3 m s^{-1} to 0.5 m s^{-1}, respectively. Their results showed that the fluid flow phenomena took the form of whirlpools or vortices that occurred between the screw blades as a consequence of a produced linear momentum. It is to be noted that the generated linear momentum was a result of the hydrostatic forces that acted against the screw blades applied in two opposite directions. Hence, the resultant forces yielded to the AST shaft's angular momentum. These vortices were analyzed to have adverse effects on the AST efficiency since most of the kinetic energy that was supposed to propel the turbine blades is diverted into these vortices between the screw blades. To minimize the effect of the vortices, it was suggested to reduce β, as they showed in their results that the highest efficiency occurred at the lowest β value in their experiment. When the λ and Fr were $1.0r_o$ and 0.12, the efficiencies recorded were at 89%, 84%, and 81% when the β were at 25°, 35°, and 45°, respectively.

Shahverdi [32] used response surface methodology (RSM) and the Buckingham Pi theorem to predict the maximum efficiency of lab-scale AST under different flow conditions. The Buckingham Pi theorem was used to model the dimensionless equation that shows the different function groups used to quantify efficiency. The derived dimensionless groups and the variables used are shown in Equations (2)–(4).

$$\eta = f_1(D_o, L, \omega, N, Q, H, \beta, \rho, \mu, g) \tag{2}$$

$$\eta = f_2\left(\frac{D_o}{H}, \frac{H}{L}, \beta, \frac{\rho\sqrt{gH^3}}{\mu}, \omega\sqrt{\frac{H}{g}}, \frac{\omega\sqrt{Q}}{(gH)^{\frac{3}{4}}}, N\right) \tag{3}$$

$$\eta = f_3\left(\frac{D_o}{H}, \beta, \Phi, N\right) \tag{4}$$

where D_o is outer diameter (m), D_i is inner diameter (m), p is screw pitch (m), L is screw length (m), ω is rotational speed (rpm), N is the number of blades, Q is the design flow rate (m^3 s^{-1}), H is the hydraulic head (m), β is screw angle inclination (°), ρ is water density (kg m^{-3}), μ is water viscosity (Pa-s), g is the gravitational acceleration (m s^{-1}), Φ is specific speed, and η is efficiency.

For the response surface methodology, β was varied from 20° to 35°, the dimensionless diameter (D_o/H) was varied from 0.435 to 0.731 by varying H from 0.200 m to 0.344 m, specific speed (Φ) was varied from 0.16 to 0.75, and the number of blades was varied from 2 to 4 [32]. The central composite design of the experiment was produced using Design Expert 11, Stat-Ease was used for statistical analysis in the computation of the regression equation, and flow3D was used for numerical simulations for creating the required response values, with Fractional Area/Volume Obstacle Representation and Volume of Fractions tools used to identify solid and liquid entities, respectively. The numerical model was validated by comparing it with experimental results from the literature. The constructed regression model from RSM and the Buckingham Pi theorem was shown to have good prediction accuracy with an R^2 of 0.9755, a p-value less than 0.0001, and a maximum relative error of 4.75%. Most considered variables were found to be significant in the regression model, such as β, D_o/H, and Φ, except for the number of blades. The efficiency value ranged from 31.6% to 83.4%, and the most optimal configuration was at a β of 27°, D_o/H of 0.731, and N of 4. The developed model is only applicable to AST designs within the range of the varied parameters of β, D_o/H, and Φ.

Lee and Lee [33] conducted a simple experimental investigation on the effects of screw angle inclination and river inlet velocity (u) on the efficiency of an existing AST prototype. However, unlike other research, the range of values for its β explored very high inclination angles ranging from 30° to 90°, while the river inlet velocity u was varied from 1.0 m s^{-1} to 1.5 m s^{-1}. The single-blade AST prototype dimensions were found to have a diameter ratio of 0.5, a pitch of 0.15 m, and a screw length of 1.56 m. The results showed that a river inlet velocity, u of 1.5 m s^{-1}, and β of 45° made for the most optimal configuration at a rotational speed of 179.8 rpm, an output brake power of 1.54 kW, and a mechanical efficiency of 94.6%.

Shahverdi et al. [34] investigated the feasibility of replacing the existing check structures in irrigation canals with an AST instead. Unlike most other research that optimized the parameters of an AST using CFD or FEM software, Shahverdi et al. optimized their numerical model in MATLAB 2013A. The developed numerical model in MATLAB used many selected empirical equations from various works in its numerical iteration, which considered the geometric parameters of the AST, calculation of ideal power and power losses, and flow leakages. In the numerical simulations, the screw length (L), screw angle inclination (β), rotational speed (ω), and the number of blades (N) were varied by 4 m to 7 m, 15° to 35°, and 1 blade to 5 blades. The optimal results of their simulation were an L of 6, β of 20°, and a single blade that generates a mechanical power of 19.9 kW and mechanical efficiency of 90.83%.

Dedić-Jandrek and Nižetić [35] experimentally investigated which AC or DC generators can produce more power when coupled to an AST. The geometric parameters of their three-bladed AST were an inner diameter (D_i) of 0.16 m, an outer diameter (D_o) of 0.30 m, and a pitch (p) of 0.3 m. For their experimental tests, they varied the screw angle inclination (β) at 21°, 25°, and 30°, and the head (H) was varied at 0.5 m, 0.55 m, and 0.61 m. Experimental results showed that the maximal efficiencies of the AST, when coupled to the AC and DC generators, were at 67% and 57% when β was 21° and H was 0.5 m.

Maulana et al. [36] performed experimental tests on their fabricated two-bladed AST prototype. The geometric parameters of their AST were mostly based on Rorres' work, wherein their AST had a screw length of 2 m, an outer diameter of 0.144 m, an inner diameter of 0.077 m, and a pitch of 0.287 m. In the experimental tests, the flow rate was varied at 90 m^3 h^{-1}, 45 m^3 h^{-1}, and 15.84 m^3 h^{-1}. Results showed that the maximal output power of 116.1 W had an efficiency of 47% at the lowest flow rate, while the highest efficiency of 55% was found at the median flow rate with a power output of 67 W. They explained that higher flow rates decreased turbine torque but increased the rotational speed, which caused the turbine to become more difficult to rotate at higher flow rates.

Betancour et al. [37] determined and verified the relationship and interactions of ductless AST geometric parameters such as diameter ratio (D_i/D_o), axle length (L), and pitch (P) to the maximal power coefficient (C_p). They have numerically simulated an AST through the use of a composite face-centered central composite design of experiment. At a significance level of 0.05, the analysis of variance (ANOVA) was used to verify the relationship and interactions of the related parameters statistically and to quantify the resulting regression model, which was a second-order quadratic model. The numerical simulations were conducted in ANSYS Fluent using a six-degrees-of-freedom transient solver. The dimensions of the rectangular fluid domain, such as the length, height, and width, were $2D_o$, $5D_o$, and $3D_o$, respectively. They utilized a constant inlet velocity of constant 1 m s^{-1}. The value ranges for the L, P, and D_i/D_o were varied between 0.30 m to 0.34 m, 0.12 m to 0.20 m, and 0.2 m to 0.6 m, and the CFD and predicted values of the maximal C_p ranged between 0.1280 to 0.5113 and 0.1205 to 0.5063, respectively. The results showed good agreement between the CFD and the predicted value accompanied by an F-ratio of 62.55 and a p-value of 2.368×10^{-7}, and the R^2 and ${R_{adj}}^2$ values were found to be

97.4% and 95.8%, respectively. The only significant parameters determined here were P and D_i/D_o, wherein the decreasing P or D_i/D_o increases C_p. They also noted that when the value of L was 0.34 m, the value of P ranging from 0.12 to 0.16 m did not significantly affect C_p. The optimal values for the geometric parameters such as D_i/D_o, L, and p were found to be 0.2, 0.12 m, and 0.30 m at a maximal C_p of 0.5063.

Similarly, another work by Bouvant et al. [10] pursued a similar study, but the screw blade angle inclination (α) was also considered. The same face-centered central composite experimental design and numerical experiment setup were used alongside the same factors and factor ranges but with the addition of α, which ranged from 60° to 80° to be tested against C_p. At a significance level of 0.05, the important parameters that significantly affected C_p were α, α*(D_i/D_o), and $(D_i/D_o)^2$, wherein increasing α increased C_p, decreasing the interaction α*(D_i/D_o) increased C_p, and decreasing the quadratic term $(D_i/D_o)^2$ increased C_p. The F-ratio, p-value, ${R_{adj}}^2$ of the regression model were 101.8, 5.319×10^{-13}, and 97.21%, respectively. The optimal values for the geometric parameters such as D_i/D_o, L, P, and α were found to be 0.1 m, 0.36 m, 0.22 m, and 73.94°, respectively, when the C_p was 0.5515.

These studies are significant to the design and development of the AST and the enhancement of its performance. Relevant studies were found in the section of literature that contributes to the improvement of the design of ASTs and are discussed as follows. One of the factors affecting the power performance of the AST is the fill level that is affected by leakages. Lubitz William et al. [47] developed a predictive model to link the parametric configuration of ASTs, the variable fill level, and leakage scenarios. On the other hand, Songin and Lubitz [48] established a method to measure an AST's fill level and leakages. Meanwhile, Dellinger et al. [49] experimentally evaluated the influence of fill level, leakages, and friction coefficient on AST performance. It was, found through the development of a power loss model by Kozyn and Lubitz [50], that the hydraulic friction and submersion of the AST outlet played a major role in the friction coefficient of AST performance. The effect of the head inflow and the angle of the turbine axis was also assessed by Saroinsong et al. [51] to a three-bladed AST. It was believed for some time by Saroinsong et al. [52] that a three-bladed AST is at its optimal when assessed together with the flowrate and the slope. Later on, the evaluation of the three-bladed AST was expanded by Saroinsong et al. [53] to establish the influence of the Froude number on the AST efficiency. Meanwhile, Simmons et al. [54] evaluated the effect of the inclination angle of ASTs on the power generation capacity at the constant head, which was found to have a recommended inclination angle of 20° to 25°. Lastly, the effect of the drive train system on the rotational speed of the AST was investigated by Suraya et al. [55], who found that the enlargement of the diameter of the pulley required lower rotational speed to generate maximum power for the system. With these AST design studies, the performance improvement in terms of power output and efficiency is documented. This is one step closer to the commercialization and installation of a large-scale AST for hydropower production [56].

4. Manufacturing Methods of Archimedes Screw Turbines

This section discusses the methods used to manufacture Archimedes screw turbines. It compiles different manufacturing methods taken from various research works and documented patents. Based on these documents on AST research, it was identified that there were four major classifications of manufacturing methods used to produce ASTs, such as traditional manufacturing, CNC manufacturing, molding manufacturing, and 3D printing. Furthermore, current works on ASTs scarcely describe the manufacturing process of the AST prototypes used in their experiments. As such, the processes described in this section were inferred from pertinent excerpts that describe AST manufacturing in their works and from patented manufacturing methods of similar machines or parts.

4.1. Traditional Manufacturing

Traditional manufacturing refers to metal-based fabrication methods to manufacture ASTs using conventional metalworking processes that have been used in the industry. This manufacturing method is mostly a type of subtractive manufacturing, which involves staged and gradual removal of material, commonly metal, from the workpiece. Unlike the straightforward flow of 3D-printing-based manufacturing, traditional manufacturing comprises multifarious processes, and several combinations of these processes can be employed to realize the final product. Research works that mentioned the use of traditional manufacturing on their AST prototypes are discussed in the following.

Rohmer et al. [39] conducted an experimental and numerical study on a manufactured AST to investigate its performance. In their study, they described the novelty of their manufacturing method. They stressed the adverse effects of welding in AST, stating that welding must be of high quality and have no defect to prevent changes in material properties that would induce corrosion in the AST. The welding process was removed from the manufacturing process by making their prototype modular to improve durability and economic life, leaving only the milling and cutting processes. Their AST design comprised a tubular core and screw blades; at least one blade was around the tubular core, and the rest were removable. The modularity of their design allowed the AST to have modifiable geometric parameters post manufacture.

Erinofiardi et al. [26] experimentally studied a manufactured AST to investigate the turbine's rotational speed and power relationship. They only mentioned that the AST was manufactured using simple manufacturing methods. A Polyvinyl chloride (PVC) pipe was used for the ducting of the turbine, while the screw blades were made of aluminum, and the screw blades were fastened to the turbine shaft using rivets; the material for the turbine shaft was not disclosed.

Abdullah et al. [40] conducted a numerical and experimental study on a manufactured AST to investigate the effect of flow rate, shaft inclination angle, and the number of screw blades on AST performance. They mentioned that their prototype was made from locally available materials, consisting of 12 screw blades welded onto a hollow turbine shaft. The screw blades were made from annular metal sheets, and these sheets were shaped into helixes using an undescribed process. The screw blades and turbine shaft were made of stainless steel, and the ducting was a galvanized iron tube with one lateral side being cut.

Durrani et al. [41] proposed the use of an AST to utilize sewage water for hydropower generation. They mentioned that the manufacturing process they used for their prototype included cutting, rolling, and welding. Galvanized metal sheets were used for ducting and the screw blades, while the material for the turbine shaft was unspecified.

Syam et al. [42] experimentally tested their manufactured AST to gauge its performance based on flow rate, torque, power, and efficiency. They showed that their prototype comprised a hollow tube shaft to which the screw blades were attached, but it was not specified if the connection was welded or fastened. It was only mentioned that the turbine utilized was made from 201 stainless steel.

Bauyon [57] designed and manufactured an AST for application in a river stream in the Philippines. They showed several processes in the manufacturing of their prototype. A vise bench was used to reshape metal sheets into screw blades, and the screw blades were fastened onto a hollow PVC pipe used as the turbine shaft.

4.1.1. Screw Blade Manufacturing

From these research works, it was inferred that traditional AST manufacturing comprises two main processes: screw blade manufacturing and assembly. The parts of the AST, the screw blade, and turbine shaft are always manufactured separately and then conjoined together through welding or fastening [58]. This method comprises several subtractive manufacturing processes to realize the helical shape of the screw blade.

The subtractive manufacturing method for the screw blade comprises punching, cutting, and reshaping or bending the metal sheets into helices. Based on the reviewed works, annular metal sheets are commonly used as the workpiece for the screw blade [40,41,57]. Annular metal can be made from metal sheets. Metal sheets are placed under punching machines, and the machine exerts shearing pressure unto the metal sheet to extrude the sheet's annular geometry, as seen in Figure 6. After obtaining the annular metal sheet, according to Abdullah et al. [40] and Durrani et al. [41], a straight cut is made on the annulus of the annular metal sheer. The purpose of this cut was to allow the annular metal to be bent in order for it to be reshaped into a helix. The reshaping of the annular metal into a helix requires the use of either a vise bench or a screw-flight-forming apparatus. Bauyon [57] used a vise bench to reshape their workpiece into a screw blade, as seen in Figure 7a. A screw-flight-forming apparatus has been shown to manufacture screw helices, which can be seen in Figure 7b [59]. The difference between the use of these two apparatuses may mostly depend on the size of the screw blade (e.g., the diameter of the screw blade) desired to be formed; vise benches have been shown to manufacture screw blades of picoscale Archimedes turbines [59], while screw-flight-forming apparatuses were shown to manufacture large screw flights. Although the use of vise bench and screw flight forming are practical methods to manufacture screw helices, these methods may also present some minute irregularities in the dimensions and shape on a component basis.

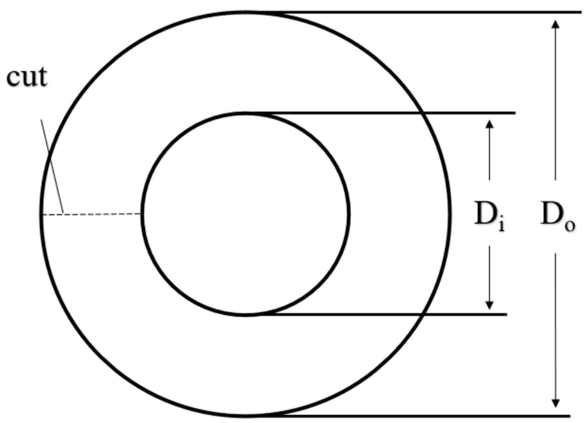

Figure 6. The annular metal diagram adopted from Abdullah et al. [40].

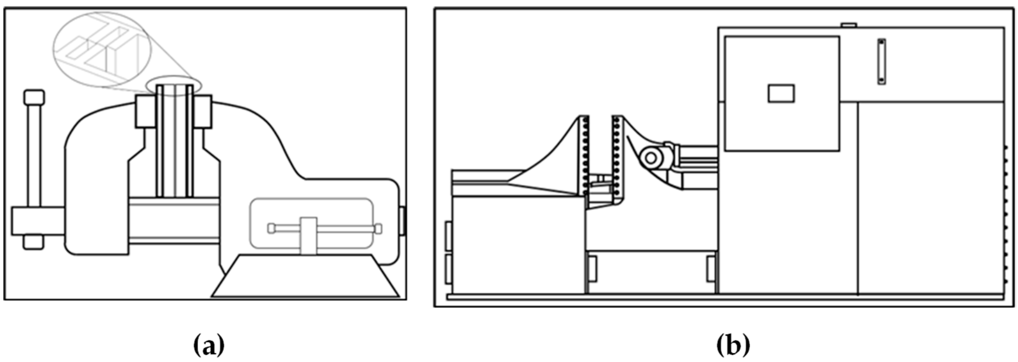

Figure 7. Apparatus used in screw blade manufacturing: (**a**) a vise bench on the left [57] and (**b**) a screw flight forming apparatus on the right [59].

Only the work of Walker et al. [60] was found to perform a life cycle assessment (LCA) on the production of AST for tidal energy conversion. The majority of the sustainability assessment of conventional methods of fabricating a turbine blade are all concentrated on wind turbines [61–64]. Thus, there is an opportunity to assess the environmental impact of conventional methods of manufacturing AST.

4.1.2. Assembly of Archimedes Screw Turbine

A wide array of easily accessible materials are available for the turbine shaft: PVC pipes, typically for plumbing applications, were used as a turbine shaft for the AST [57], and manufacturers can provide various sizes of shafts for the AST. After manufacturing the screw blades and the turbine shaft, the screw blades are attached to the turbine shaft through either welding or fastening based on the reviewed research works [39]. Hindle and Boersma [65] discussed in their patent on the AST that the screw blade is welded onto the turbine shaft. However, there has been no direct comparison between the two methods of attaching the screw blades, but respective advantages have been mentioned. As previously stated, Rohmer et al. [39] discussed the adverse effects of welding on ASTs. On the other hand, fastening by rivets does not have these adverse effects. However, leakage losses can occur since this process does not close the air gaps between the screw blades and the turbine shaft. Therefore, the tradeoff between the adoption of welding over fastening is the avoidance of leakage losses versus susceptibility to corrosion.

4.2. CNC Manufacturing

Manufacturing techniques of computerized numerical control (CNC) machines have not yet been documented for AST manufacturing, but research on the manufacturing of similarly helical-shaped objects has been found. CNC machining is a type of subtractive manufacturing method that uses computerized control to automatically move a working (e.g., rotating) tool that removes metal from a workpiece with very high precision. Programming using NC code is inputted to the controlling unit, which controls the motion of the tool around the workpiece.

Bizzarri and Bartoň [66] highlighted flank machining with the use of CNC machines in manufacturing screw rotors. They mentioned that manufacturing screw rotors is a complex process that requires expensive machinery, and the working tool conventionally makes several passes over a tool path. To optimize this manufacturing process, a specialized approach using a five-axis flanking machine with double-flanking for manufacturing screw rotors was proposed. In this approach, an appropriate shape for the working tool was determined, and the tool's motion was optimized. All proof and computations were conducted using numerical experiments.

Matejic et al. [67] emphasized the improvements in the CNC machining of progressive screw shafts. The manufacturing of progressive screw shafts using CNC lathe machines and three-axis CNC milling machines had severe limitations. To resolve these limitations, they added a fourth axis to the three-axis CNC milling machine, and they used Autodesk Inventor HSM software for the controlling unit of the CNC machine. With these technological upgrades, the CNC machine can now flexibly manufacture varying designs of progressive screw shafts without custom-shaped tools and complicated functions of the machine.

Although CNC manufacturing has a significant contribution to the production of screw rotors, no research articles were found that used CNC machining to generate an AST. Moreover, no LCA studies were found that evaluated the CNC machining of AST. However, Swetha et al. [68] performed a comparative gate-to-gate LCA on conventional manufacturing via CNC machining and additive manufacturing for a sprocket adapter. Their results revealed that additive manufacturing had a lesser environmental impact compared with conventional manufacturing, such as the CNC machining approach [68].

4.3. Molding Manufacturing

Another method for manufacturing screw blades is conducted through the use of the molding process. A method for using the molding process for forming screw flights was invented by Lapeyre [69]. Molding processes are additive manufacturing techniques that require pouring molten metal or plastic resin into the cavities of specially made casts whose cavities are exactly shaped to the geometry of the desired product [70]. The final product is realized after the molten material temperature cools down and the material solidifies into a mold [71]. Similarly, in a patent for the invention of the AST, Hindle and Boersma [67] outlined the use of molding for manufacturing the AST screw blades. The specific molding processes for ASTs involve injection molding and rotary molding casting. Limited studies are available on these types of manufacturing processes, specifically on ASTs. However, Atkin [58] has used light resin transfer molding to manufacture an industrial AST. It is to be noted that the study considered the comparative evaluation of different manufacturing methods of the screw blade. The results determined that light resin transfer molding was the preferred method in manufacturing the ASTs [58]. It was highlighted that the composite material used in the manufacturing of the AST provided an almost comparable structural performance to steel. Moreover, it was outlined that the composite material is relatively lighter, corrosion-resistant, and provides less friction than steel [58].

No LCA study was found to evaluate the environmental impact of manufacturing an AST using the molding process. The nearest LCA study on the turbine molding process is the work by Upadhyayula et al. [72], which was applied to wind turbines. The functional unit they utilized is a three-blade, off-shore wind turbine. The results showed that the recycled carbon fiber used in the molding process had the optimum environmental impact when compared to the use of virgin carbon fiber. To further understand the impact of the molding process in the life cycle of the AST, an LCA study is suggested.

4.4. 3D Printing

3D printing is a relatively modern technique used in the manufacturing industry that has been reliable in manufacturing products with high precision [73]. It is a form of additive manufacturing in which material is continually added to the workpiece to realize the final product. The physical dimensions of a product are first realized into a CAD model, which generates an STL file format (standard triangulation language) that the 3D printer uses to manufacture the desired product by additively building it with appropriate material [74]. Several researchers have stated that they have used 3D printing to manufacture their AST prototype.

Dellinger et al. [24] studied the structure of 3D turbulent flows and energy losses in the screw of an AST by finding the coefficients within turbulent closure models. They developed a CFD model and manufactured a laboratory-scale AST prototype to compare the results. For the manufacturing method, they only mentioned that the whole prototype was manufactured with Acrylonitrile butadiene styrene (ABS) plastic using a 3D printer.

Zitti et al. [38] performed numerical simulations and experimental investigations of a ductless AST to investigate its efficiency. Their AST prototype's screw and shaft were manufactured separately using a 3D printer, and both materials were made of polylactic acid (PLA). The parts were then conjoined together using high-performance glue.

Sari et al. [75] presented a review of the various characteristic performances of different AST research works. In one citation, they showed a feasibility study that was carried out on using a 3D-printing machine for manufacturing screws using PLA and epoxy. Their findings were that screws manufactured using PLA and epoxy were cheaper than metal-based manufacturing, but they also warned that PLA-based screws were only reliable for two years.

Shashank et al. [74] theoretically and empirically investigated the performance of a 3D-printed AST prototype. They chose PLA for the material of the AST prototype based on its mechanical properties that are desirable for hydropower generation, namely, melting point, tensile strength, cost, and biodegradability, which make it environment friendly. The CAD model of the prototype comprised the whole AST, and the AST was manufactured using a 3D printer.

A couple of studies were found to have used the 3D-printing method to manufacture ASTs. Straalsund Jerry et al. [76] employed 3D-printing technology to generate various shapes of ASTs for a comparative experimental investigation of various blade shapes, such as strake, reverse strake, and helicoid. On the other hand, Lee et al. [77] utilized the 3D-printing technology via fused deposition modeling to manufacture the controllable pitch blades of the AST. With the use of the 3D-printing manufacturing approach, unconventional blade shapes can be considered for the AST.

Based on these research works, the manufacturing process of ASTs using 3D printing is straightforward. The designer must first determine if the screw blade and shaft of the AST are to be manufactured separately or conjointly. This aspect will affect all downstream processes associated with the manufacturing of the AST. For prototypes in separate parts, CAD models for both screw blades and the shaft will have to be made, and they will have to be conjoined together using high-performance adhesive after 3D printing. For prototypes in one whole entity, a single CAD model is required to be able to generate the 3D-printed model of the AST.

Although 3D printing of turbine blades provides advantages, such as flexibility of the design and consideration of more complex blade configuration, it should be noted that it consumes thermoplastic materials that can cause environmental impacts. These environmental impacts can have an exponential effect on large-scale systems. Recently, Olivera et al. [78] highlighted that the detrimental environmental impact of the utilization of 3D-printed turbine blades reside in the recycling process. This is due to the fact that the thermoset materials used in the 3D-printing process contain fibers that are challenging to recycle while their thermo-mechanical properties degrade [79]. Meanwhile, Serra et al. [80] performed a comparative LCA between additive manufacturing, a type of 3D printing, and precision casting of gas turbines. Their results indicated that additive manufacturing is a relatively sustainable process compared to precision casting, with greenhouse gas emissions being lower by 40% [80]. Additionally, Torres-Carrillo et al. [81] also conducted a comparative cradle-to-gate LCA between selective laser melting, a kind of 3D printing, and investment casting on aeronautical turbine blades. The results of their study revealed that the carbon footprint of additive manufacturing is 4% lower compared to investment casting [81]. With the beneficial environmental results of the 3D-printing process compared with other blade manufacturing processes on different turbine blades, it is suggested that 3D printing be used for ASTs.

5. Challenges and Future Perspective

With the establishment of the optimal design parameters of the AST from previous works, it was also found that the two main manufacturing methods of ASTs are conventional manufacturing and 3D printing. The enhancement in its manufacturability is a vital success component of using the technology to further improve the adoption of ASTs in potential hydropower sites. Hence, it is important to identify the challenges in their manufacturability. The challenges of these manufacturing methods of ASTs and their future perspective are discussed in this section.

5.1. Discussion of Optimal Geometric Parameters

Several geometric parameters that appear to be significant for ASTs are the diameter ratio, the number of blades, screw pitch, screw length, the screw inclination angle, and the filling factor.

The AST research community generally accepts Rorres' [7] work on the optimum diameter ratio of 0.54, as many research works have used it in their studies as a standard [10]. Further studies on this subject appear to be unnecessary.

The explored range of the number of blades on AST is one to five, and five blades were shown to have the highest output power [25]. However, the extra blades on AST incur higher manufacturing costs, and some researchers have selected one or two blades for their AST as a result [32,34]. The optimum number of blades on the AST is still a matter of discussion, as no work extensively investigated the trade-off between power output and manufacturing costs.

There is no set of standards for screw pitch, and only one study has investigated its effects on efficiency so far. Simmons et al. [28] quantified the optimum screw pitch in the form of a pitch–diameter ratio and prescribed a pitch–diameter ratio of 1.0.

The optimal screw length differs on a site-to-site basis, trading off between power output and the structural bending load, friction losses, and heavier manufacturing cost on the screw [28]. A low-inclination AST tends to have longer screws, while a higher-inclination AST is inclined to have shorter screws. Even though higher-inclination ASTs have a relatively shorter length, they have been shown to reach high efficiencies almost at par with small-inclination ASTs [30]. Further study on the consideration of the manufacturing cost to the feasibility of the AST design is imperative.

The community appears to accept that the optimal screw angle inclination range is 20 to 25° [43,54]. However, in one of the studies, it was shown that the optimal inclination angle was shown to vary with the number of blades on the AST; for three-blade, four-blade, and five-blade, it was 15°, 20°, and 25°, respectively [25]. The actual range of optimal screw-angle inclination elevates when the number of blades is increased. However, the alternate optimum can also be used when small-angle inclinations are too impractical (e.g., in the case of the screw being too long). It was demonstrated that high-angle inclination ASTs could reach the same efficiencies as small-angle inclination ASTs [30], where one study found the optimal value for a range of high-angle inclination (30 to 90°) to be 45° [33]. Investigation of the effects of the number of blades on high-angle inclinations is recommended for future study.

The filling factor was prescribed at 85% since higher filling factors (or design flow rates) start to incur hydraulic losses [29]. Other studies also support this claim and one observed the highest efficiency occurred at the median flow rate [36], while the lowest efficiency was observed at the highest flow rate [43].

5.2. Current Limitation of 3D-Printing Manufacturing

Table 3 shows the various performance and geometric parameters of the various AST prototypes manufactured from the reviewed research works. According to Yoosefdoost and Lubitz [4] and Suraya et al. [20], micro-hydropower plants ranged from 5 kW to 100 kW, while picoscale hydropower plants ranged from anything below 5 kW. Based on the power outputs of the AST prototypes, all manufactured prototypes are picoscale. The power output of 3D-printed prototypes ranges from 30 mW to 100 W, while traditionally manufactured prototypes in this review range from 100 mW to 3 kW. (It is widely known that ASTs normally operate at a microscale, based on a survey of more than 400 AST powerplants measured in Europe [45]). However, the lack of information on the manufacturing method from previous works limits the data on the manufacturability of ASTs. This shows that the majority of the studies were more inclined to employ 3D-printing methods on smaller-scale prototypes. It is to be noted that conventional manufacturing methods were also used in relatively larger-scale prototypes of AST. It has been established that the precision of 3D printing is advantageous in the application of nanoscale technology [82,83]. However, these results from the review show that there is some limitation in 3D-printing technology that has made it impractical on larger-scale ASTs, as opposed to traditional manufacturing, which is more attuned to larger-scale applications. This is due to the limitation of the thermoset material used for 3D printing, where its thermo-mechanical properties decline with its frequency of recycling [79]. To address this limitation, a new approach of 3D printing has been developed, employing thermoplastic extrusion- or material extrusion-based additive manufacturing (MEX-AM) [84]. MEX-AM is considered to be a technique to extract parts out of various materials such as ceramics or metals, enabling a more stable structural integrity [85] while keeping the cost per part at a minimum [86].

Table 3. Performance and geometric parameters of AST prototypes with included manufacturing details from reviewed research works.

References	Manufacturing Method	Material	Head (m)	Outer Radius (mm)	Length (m)	Power (W)	Scale
Rohmer et al. [39]	Traditional Manufacturing	–	0.8	–	–	200–3000	Pico
Erinofiardi et al. [26]		Aluminum	–	53	0.7	0.1–0.3	Pico
Abdullah et al. [40]		Stainless steel	–	65	1.0	1.5–2.5	Pico
Durrani et al. [41]		Galvanized iron	1.5	600	3.4	2000	Pico
Syam et al. [42]		Stainless steel	1.0	130	2.9	110	Pico
Bauyon [57]		–	–	–	–	200	Pico
Sari et al. [75]	3D Printing	PLA	0.4	–	–	123	Pico
Dellinger et al. [24]		ABS	–	96	–	1–3	Pico
Zitti et al. [38]		PLA	–	50	0.32	30×10^{-3}–50×10^{-3}	Pico
Shashank et al. [74]		PLA	0.1	50	–	1–5	Pico

5.3. Advantages and Disadvantages of Manufacturing Methods

Each manufacturing method has its nuances that imply its economic feasibility. Rohmer et al. [39] previously stated that manufacturing a screw blade is difficult from an industrial point of view, which is opposed to other references that claim ASTs are simple to manufacture [9,11]. They stated that AST manufacturing requires several skills needed to realize the prototype, namely, milling, cutting, and welding, which, according to them, are not readily available skills. Durrani et al. [41] stated as well that several processes were also involved in the manufacturing of their prototype. As opposed to traditional manufacturing, 3D printing does not require multifarious skills in different processes, as the 3D-printing process is straightforward: generation of the CAD model and computer-assisted actuation of the 3D printer. This implies that traditional manufacturing is more skill-intensive than 3D printing.

On the other hand, 3D printing is disadvantaged in terms of material selection. Shashank et al. [74] outlined that the use of PLA plastic as the material for 3D-printed ASTs has fewer adverse effects in the environment compared to metal-based materials since PLA is biodegradable. Sari et al. [75] highlighted that PLA material for 3D printing is less expensive than metal-based manufacturing. However, they further stated that PLA material is less durable and that it only has an economic life of two years for AST prototypes. Dezaki et al. [87] compared the two methods and stated that the advantage of traditional manufacturing over 3D printing is material strength and selection. Therefore, AST prototypes using traditional manufacturing are expected to last longer than prototypes made using 3D printing.

5.4. Design for Manufacturability

The design for manufacturability (DfM) aims to effectively produce a product that simplifies the manufacturing process that essentially reduces the cost while satisfying the design and distribution constraints [88]. Very few studies have employed DfM in the fabrication of turbine technologies. Tessarolo et al. [89] applied DfM to develop an off-shore direct-drive wind turbine, while Premkumar et al. [90] developed a semantic knowledge management system that utilized DfM concepts for the fabrication of wind turbine blades. On the other hand, Pietropaoli et al. [91] proposed the design for an additive manufacturing approach for the production of complex gas turbine components. No studies were observed to apply the DfM concept to ASTs.

5.5. Recommendation for Future Works

Future works can work on quantitative analysis of manufacturing ASTs' economic and logistical aspects. Currently, there are no concrete data on the costs of manufacturing, installment, and maintenance of ASTs. A cost–benefit economic analysis is also suggested to ascertain the trade-offs between traditional manufacturing and 3D printing. For the 3D-printing process, it is recommended to explore the use of the MEX-AM approach, as it has the potential for the production of large-scale components, such as AST [92]. Statistical assessments of possible manufacturers and sources of skills for ASTs manufacturing will be helpful in the logistical aspect, as they can be a precursor to the feasibility and sustainability of AST manufacturing. One possible avenue of research is to apply multicriteria decision methods (MCDM), such as fuzzy logic-based methods [93] or the analytical hierarchy process [94], on the material selection for ASTs. MCDMs are useful in determining the optimal solution based on several criteria that define optimality; for hydroturbines, these could be material density, toughness, weldability, corrosion resistance, durability, and expenses incurred.

Most of the works cited in this review paper are available in the literature for access. It is possible that most research on AST is written in foreign language aside from the English language, given the low research volume of AST research, as illustrated in Figure 2. Thus, gaining access to these documents can shed light on the manufacturability of ASTs and can aid as additional parameters to guide the design process of AST.

Very few sustainability assessment studies were found on the LCA and the techno-economic analysis (TEA) of the AST. Kathwadia et al. [95] performed a cradle-to-grave LCA to determine the environmental impacts of the manufacturing stages of conventional turbine blades. Their study also assessed the influence of variability on the used turbine components. Meanwhile, Walker and Thies [96] employed a cradle-to-dock, dock-to-grave LCA to compare the different materials for the production of the tidal turbine blades. Their study revealed that glass fiber blades have a relatively lower environmental impact compared to steel and carbon fiber blades. [96]. On the other hand, Walker et al. [60] conducted a comparative LCA study of various tidal energy conversion turbine technologies, including ASTs, where a functional unit of 10 MW output was used. Their results indicate a carbon dioxide intensity ranging from 18 to 35 gCO_2 KW^{-1}-h^{-1} and a payback period of 12 years for all technologies [60]. Meanwhile, only a few studies were found that covered the TEA of AST and are discussed as follows. Oliveira et al. [97] assessed the hydropower-harvesting capacity of ASTs at the Alviela River in Portugal using the TEA, where it was found that the payback period for an investment of EUR 160,000 and an internal rate of return of more than 10% is about 8 years. Ceran et al. [98] compared the TEA of AST and Kaplan turbines in terms of levelized cost of electricity and the net present value for low-head sites. They found that the minimum head is only sensitive to the AST compared to the Kaplan turbine. Moreover, the decline in the power production due to the minimum head of the site for ASTs does not exceed 52% [98]. A recent sustainability assessment approach was developed by Musacchio et al. [99] that integrated LCA with the company's costs analysis that enabled the evaluation of materials and manufacturing techniques of a gas turbine. Moreover, Miklautsch et al. [100] proposed harmonizing Industry 4.0 technologies to automate the manufacturing methods with LCA in production companies. Industry 4.0 enables the use of smart materials, smart factories, and smart supply chains to optimize materials wastage, minimize inventory, and minimize operational costs [101]. These LCA and TEA studies are indicative of the sustainability of typical turbine blades for renewable energy production. The advent of Industry 4.0 plays a major role in utilizing automation technologies and monitors, in real-time key, sustainability indicators. However, the intricate design and complexity of the AST cause the manufacturability challenges. Hence, comprehensive sustainability assessments through LCA and TEA studies are recommended for ASTs, including the application of the Industry 4.0 framework.

Recently, only two studies employed the use of artificial intelligence (AI) in the performance of ASTs. Paturi et al. [102] employed an artificial neural network (ANN) coupled with CFD to predict the power coefficient of the AST. Moreover, their results indicated that the diameter ratio is highly sensitive to the power performance of the AST [102]. On the other hand, Kozyn et al. [103] also utilized an ANN to predict the power output of ASTs using numerical experimental data from the field- and laboratory-scale. Their results showed an ANN prediction model of AST power output with an accuracy of 94% [104]. Future work can focus on the development of an AI linking the design and manufacturability of the AST to its power output performance and its sustainability.

In terms of the optimal design of ASTs, various design methods and models were implemented in the past. Lisicki et al. [104] employed a Bayesian optimization model to design and configure an AST for specific applications. Moreover, a rapid estimation model was recently developed by Yoosefdoost and Lubitz [105] to design and configure an AST to accelerate the design process and minimize the cost of production for a specific site installation. Currently, these studies lack the consideration of the manufacturing process. By developing an optimization model or a rapid estimation model that incorporates the manufacturability of the AST, an AST design can easily be generated that minimizes the cost and identifies the appropriate manufacturing process for a specific location. Moreover, the DfM presents a cost-efficient way to manufacture complex turbine systems such as ASTs. Thus, it is recommended to be employed in future AST projects.

6. Conclusions

A systematic approach to the critical review of the manufacturability of AST for renewable energy is presented in this work. This review paper presented an assessment of the bibliometric scope of manufacturability in AST research. In addition, the study was also able to determine and differentiate the various methods of manufacturing AST. The bibliometric review showed that there is scarcely any mention of the manufacturing of AST in the available literature. It was found that recent research works on AST and relevant reviews on AST lack discussion about manufacturing methods. The significant geometric parameters of AST were determined to be diameter ratio, screw length, screw pitch, screw angle inclination, number of blades, and filling factor, and their respective optimum values were discussed. The studies revealed that 3D-printed AST had power outputs of 3 mW to 123 W, while reported, traditionally manufactured turbines had power outputs of 100 mW to 3 kW. Further improvements in 3D printing could possibly make it applicable at the micro-hydroscale. Traditional manufacturing of AST is more skill-intensive and difficult to conduct, while 3D printing results in the lower economic life of AST. CNC manufacturing was found to produce screw rotors successfully. However, limited studies were found that employed CNC manufacturing to AST. Therefore, there is a considerable lack of manufacturing information that could clarify the economic value of AST manufacturing, which can bridge the research gap in optimal design criteria and manufacturing costs. Future works include a comparative sustainability assessment of the manufacturability of AST in terms of economic, social, and environmental aspects. Various approaches in the design of AST must be explored in the future that incorporate the manufacturability of AST, such as artificial intelligence, computational fluid dynamics, optimization techniques, rapid estimation models, and design for manufacturability. Moreover, thermoplastic extrusion-based additive manufacturing is suggested to be explored for the large-scale production of ASTs.

Author Contributions: Conceptualization, A.T.U., I.A.V.M.III, M.S.P. and C.L.S.; methodology, A.T.U., I.A.V.M.III and A.M.A.C.; software, M.S.P. and C.L.S.; validation, A.T.U., I.A.V.M.III, M.S.P., C.L.S. and W.-H.C.; formal analysis, A.M.A.C. and A.T.U.; investigation, A.M.A.C.; resources, A.T.U., I.A.V.M.III, M.S.P. and C.L.S.; data curation, A.T.U., I.A.V.M.III and A.M.A.C.; writing—original draft preparation, A.M.A.C.; writing—review and editing, A.T.U., I.A.V.M.III, M.S.P., C.L.S. and W.-H.C.; visualization, A.T.U., I.A.V.M.III and A.M.A.C.; supervision, A.T.U.; project administration, A.T.U.; funding acquisition, A.T.U., I.A.V.M.III, M.S.P. and C.L.S. All authors have read and agreed to the published version of the manuscript.

Funding: The study is funded by the Research and Grants Management Office of the De La Salle University (DLSU) with project number "03 IR U 1TAY20-1TAY21". This research is also partly supported by the Higher Education Sprout Project, Ministry of Education, who aided the Headquarters of University Advancement at National Cheng Kung University (NCKU). Lastly, the APC was funded by the Research Dissemination Grant of Engineering Research and Development for Technology of the Department of Science and Technology, Philippines.

Institutional Review Board Statement: The study was conducted in accordance to the University Ethics Regulations of De La Salle University and was approved by the Review Ethics Review Board of De La Salle University.

Informed Consent Statement: Not applicable.

Data Availability Statement: Not applicable.

Acknowledgments: The authors acknowledge the financial and deloading support from the Research and Grants Management Office of the De La Salle University (DLSU) with project number "03 IR U 1TAY20-1TAY21". The last author is grateful for the support provided by the Higher Education Sprout Project, Ministry of Education to the Headquarters of University Advancement at National Cheng Kung University (NCKU). The authors acknowledge the Research Dissemination Grant of Engineering Research and Development for Technology (ERDT) of the Department of Science and Technology (DOST), Philippines, for the financial support to cover the APC.

Conflicts of Interest: The authors declare no conflict of interest.

Nomenclature

Parameters	**Archimedes Screw Turbine**
r_o	outer radius (mm)
D_o	outer diameter (mm)
D_i	inner diameter (mm)
ω	rotational speed (rpm)
P	screw pitch (m)
L	screw length (m)
N	number of blades
Q	design flow rate(m^3/s)
H	hydraulic head (m)
ρ	water density (kg/m^3)
μ	water viscosity (Pa-s)
u	inflow velocity (m/s)
β	screw angle inclination (°)
α	screw blade angle inclination (°)
g	gravitational acceleration (m^2/s)
Φ	specific speed
λ	characteristic length
F_r	Froude number
η	efficiency
R	coefficient of determination
R_{adj}	adjusted coefficient of determination
RSM	response surface methodology
DOE	Department of Energy
NEA	National Electrification Administration
CFD	computational fluid dynamics
CAD	computer-aided design
AC	alternating current
DC	direct current
PLA	polyactid acid
PVC	polyvinyl chloride
MCDM	multicriteria decision method

References

1. IEA. *World Energy Outlook*; IEA: Paris, France, 2022; CC BY NC SA 4.0 (Annex A). Available online: https://www.iea.org/reports/world-energy-outlook-2022 (accessed on 1 October 2022).
2. Liu, X.; Xiao, S.; Pan, H.; Zheng, X.; Han, W.; Huang, C.; Deng, S. Optimizing hydropower plants based on carbon-water-energy-ecosystem nexus. *Energy Convers. Manag.* **2022**, *270*, 116191. [CrossRef]
3. Aviso, K.B.; Marfori, I.A.V.; Tan, R.R.; Ubando, A.T. Optimizing abnormal operations of off-grid community utility systems with fuzzy P-graph. *Energy* **2020**, *202*, 117725. [CrossRef]

4. YoosefDoost, A.; Lubitz, W.D. Archimedes Screw Turbines: A Sustainable Development Solution for Green and Renewable Energy Generation—A Review of Potential and Design Procedures. *Sustainability* **2020**, *12*, 7352. [CrossRef]
5. Waters, S.; Aggidis, G.A. Over 2000 years in review: Revival of the Archimedes Screw from Pump to Turbine. *Renew. Sustain. Energy Rev.* **2015**, *51*, 497–505. [CrossRef]
6. Koetsier, T.; Blauwendraat, H. The Archimedean Screw-Pump: A Note on Its Invention and the Development of the Theory. In *International Symposium on History of Machines and Mechanisms*; Springer: Dordrecht, The Netherlands, 2004; pp. 181–194.
7. Rorres, C. The Turn of the Screw: Optimal Design of an Archimedes Screw. *J. Hydraul. Eng.* **2000**, *126*, 72–80. [CrossRef]
8. Shahverdi, K.; Loni, R.; Maestre, J.M.; Najafi, G. CFD numerical simulation of Archimedes screw turbine with power output analysis. *Ocean Eng.* **2021**, *231*, 108718. [CrossRef]
9. Simmons, S.C.; Elliott, C.; Ford, M.; Clayton, A.; Lubitz, W.D. Archimedes screw generator powerplant assessment and field measurement campaign. *Energy Sustain. Dev.* **2021**, *65*, 144–161. [CrossRef]
10. Bouvant, M.; Betancour, J.; Velásquez, L.; Rubio-Clemente, A.; Chica, E. Design optimization of an Archimedes screw turbine for hydrokinetic applications using the response surface methodology. *Renew. Energy* **2021**, *172*, 941–954. [CrossRef]
11. Hoffstaedt, J.P.; Truijen, D.P.K.; Fahlbeck, J.; Gans, L.H.A.; Qudaih, M.; Laguna, A.J.; De Kooning, J.D.M.; Stockman, K.; Nilsson, H.; Storli, P.T.; et al. Low-head pumped hydro storage: A review of applicable technologies for design, grid integration, control and modelling. *Renew. Sustain. Energy Rev.* **2022**, *158*, 112119. [CrossRef]
12. Zhou, D.; Deng, Z. Ultra-low-head hydroelectric technology: A review. *Renew. Sustain. Energy Rev.* **2017**, *78*, 23–30. [CrossRef]
13. Mueller, M.; Knott, J.; Pander, J.; Geist, J. Experimental comparison of fish mortality and injuries at innovative and conventional small hydropower plants. *J. Appl. Ecol.* **2022**, *59*, 2360–2372. [CrossRef]
14. Piper, A.T.; Rosewarne, P.J.; Wright, R.M.; Kemp, P.S. The impact of an Archimedes screw hydropower turbine on fish migration in a lowland river. *Ecol. Eng.* **2018**, *118*, 31–42. [CrossRef]
15. Renardy, S.; Colson, D.; Benitez, J.-P.; Dierckx, A.; Goffaux, D.; Sabbe, J.; Rabouan, A.; Detrait, O.; Nzau Matondo, B.; Sonny, D.; et al. Migration behaviour of Atlantic salmon smolts (*Salmo salar* L.) in a short and highly fragmented gravel-bed river stretch. *Ecol. Freshw. Fish* **2022**, *31*, 499–514. [CrossRef]
16. Pauwels, I.S.; Baeyens, R.; Toming, G.; Schneider, M.; Buysse, D.; Coeck, J.; Tuhtan, J.A. Multi-Species Assessment of Injury, Mortality, and Physical Conditions during Downstream Passage through a Large Archimedes Hydrodynamic Screw (Albert Canal, Belgium). *Sustainability* **2020**, *12*, 8722. [CrossRef]
17. Renardy, S.; Benitez, J.-P.; Tauzin, A.; Dierckx, A.; Nzau Matondo, B.; Ovidio, M. How and where to pass? Atlantic salmon smolt's behaviour at a hydropower station offering multiple migration routes. *Hydrobiologia* **2020**, *847*, 469–485. [CrossRef]
18. Simmons, S.C.; Lubitz, W.D. Archimedes screw generators for sustainable micro-hydropower production. *Int. J. Energy Res.* **2021**, *45*, 17480–17501. [CrossRef]
19. Waters, S.; Aggidis, G. Tidal range technologies and state of the art in review. *Renew. Sustain. Energy Rev.* **2016**, *59*, 514–529. [CrossRef]
20. Suraya, A.N.; Ammar, N.M.M.; Kulthum, J.U. The effect of substantive parameters on the efficiency of Archimedes screw microhydro power: A review. *IOP Conf. Ser. Mater. Sci. Eng.* **2015**, *100*, 012030. [CrossRef]
21. Poosti, A.; Lewis, F.M.; Sereno, D.; Redd, K.; Abkian, V. Time for a checkup? *Water Environ. Technol.* **2003**, *15*, 66–69.
22. Siswantara, A.I.; Warjito; Budiarso, B.; Harmadi, R.; Syafei, M.H.; Adanta, D. Investigation of the α angle's effect on the performance of an Archimedes turbine. *Energy Procedia* **2019**, *156*, 458–462. [CrossRef]
23. Ekström, R.; Ekergård, B.; Leijon, M. Electrical damping of linear generators for wave energy converters—A review. *Renew. Sustain. Energy Rev.* **2015**, *42*, 116–128. [CrossRef]
24. Dellinger, G.; Garambois, P.-A.; Dellinger, N.; Dufresne, M.; Terfous, A.; Vazquez, J.; Ghenaim, A. Computational fluid dynamics modeling for the design of Archimedes Screw Generator. *Renew. Energy* **2018**, *118*, 847–857. [CrossRef]
25. Dellinger, G.; Simmons, S.; Lubitz, W.D.; Garambois, P.-A.; Dellinger, N. Effect of slope and number of blades on Archimedes screw generator power output. *Renew. Energy* **2019**, *136*, 896–908. [CrossRef]
26. Erinofiardi, E.; Syaiful, M.; Prayitno, A. Electric Power Generation from Low Head Simple Turbine for Remote Area Power Supply. *J. Teknol.* **2015**, *74*, 5. [CrossRef]
27. Lashofer, A.; Kaltenberger, F.; Kaltenberger, F. Does the Archimedean Screw Turbine Stand the Test? In *Wasserkraftprojekte: Ausgewählte Beiträge aus der Fachzeitschrift WasserWirtschaft*; Heimerl, S., Ed.; Springer Fachmedien: Wiesbaden, Germany, 2013; pp. 310–318.
28. Simmons, S.; Songin, K.; Lubitz, W. Experimental Investigation of the Factors Affecting Archimedes Screw Generator Power Output. *HYDRO*. Available online: https://scottsimmons.ca/wp-content/uploads/2021/07/Preprint-2017-ASG-Experiments.pdf (accessed on 1 October 2022).
29. Alonso-Martinez, M.; Suárez Sierra, J.L.; Coz Díaz, J.J.D.; Martinez-Martinez, J.E. A New Methodology to Design Sustainable Archimedean Screw Turbines as Green Energy Generators. *Int. J. Environ. Res. Public Health* **2020**, *17*, 9236. [CrossRef] [PubMed]
30. Edirisinghe, D.S.; Yang, H.-S.; Kim, M.-S.; Kim, B.-H.; Gunawardane, S.P.; Lee, Y.-H. Computational Flow Analysis on a Real Scale Run-of-River Archimedes Screw Turbine with a High Incline Angle. *Energies* **2021**, *14*, 3307. [CrossRef]
31. Saroinsong, T.; Soenoko, R.; Wahyudi, S.; Sasongko, M. Fluid Flow Phenomenon in a Three-Bladed Power-Generating Archimedes Screw Turbine. *J. Eng. Sci. Technol. Rev.* **2016**, *9*, 72–79. [CrossRef]

32. Shahverdi, K. Modeling for prediction of design parameters for micro-hydro Archimedean screw turbines. *Sustain. Energy Technol. Assess.* **2021**, *47*, 101554. [CrossRef]
33. Lee, M.D.; Lee, P.S. Modelling the energy extraction from low-velocity stream water by small scale Archimedes screw turbine. *J. King Saud Univ.-Eng. Sci.* **2021**. [CrossRef]
34. Shahverdi, K.; Loni, R.; Ghobadian, B.; Gohari, S.; Marofi, S.; Bellos, E. Numerical Optimization Study of Archimedes Screw Turbine (AST): A case study. *Renew. Energy* **2020**, *145*, 2130–2143. [CrossRef]
35. Dedić-Jandrek, H.; Nižetić, S. Small scale archimedes hydro power plant test station: Design and experimental investigation. *J. Clean. Prod.* **2019**, *231*, 756–771. [CrossRef]
36. Maulana, M.I.; Syuhada, A.; Kurniawan, R. Experimental Study on the Effect of Flow rate on the Performance of Two-Blade Archimedes Screw Turbine. *J. Adv. Res. Fluid Mech. Therm. Sci.* **2020**, *61*, 10–19.
37. Betancour, J.; Velásquez, L.; Jaramillo, L.Y.; Chica, E.; Rubio-Clemente, A. Application of a central composite face-centered design in the optimization of an archimedean hydrokinetic turbine. *Renew. Energy Power Qual. J.* **2021**, *19*, 418–422. [CrossRef]
38. Zitti, G.; Fattore, F.; Brunori, A.; Brunori, B.; Brocchini, M. Efficiency evaluation of a ductless Archimedes turbine: Laboratory experiments and numerical simulations. *Renew. Energy* **2020**, *146*, 867–879. [CrossRef]
39. Rohmer, J.; Knittel, D.; Sturtzer, G.; Flieller, D.; Renaud, J. Modeling and experimental results of an Archimedes screw turbine. *Renew. Energy* **2016**, *94*, 136–146. [CrossRef]
40. Abdullah, O.S.; Kamel, A.H.; Khalil, W.H. Numerical and Experimental Modelling of Small Hydropower Turbine. *J. Adv. Res. Fluid Mech. Therm. Sci.* **2021**, *80*, 112–127. [CrossRef]
41. Durrani, A.M.; Mujahid, O.; Uzair, M. Micro Hydro Power Plant using Sewage Water of Hayatabad Peshawar. In Proceedings of the 2019 15th International Conference on Emerging Technologies (ICET), Peshawar, Pakistan, 2–3 December 2019; pp. 1–5.
42. Syam, I.; Maulana, M.; Syuhada, A. Design and Performance of Archimedes Single Screw Turbine as Micro Hydro Power Plant with Flow Rate Debit Variations (Case Study in Air Dingin, Samadua-South Aceh). *J. Inotera* **2019**, *4*, 13. [CrossRef]
43. Thakur, N.K.; Thakur, R.; Kashyap, K.; Goel, B. Efficiency enhancement in Archimedes screw turbine by varying different input parameters–An experimental study. *Mater. Today Proc.* **2022**, *52*, 1161–1167. [CrossRef]
44. Simmons, S.C.; Lubitz, W.D. Analysis of internal fluid motion in an Archimedes screw using computational fluid mechanics. *J. Hydraul. Res.* **2021**, *59*, 932–946. [CrossRef]
45. Lashofer, A.; Hawle, W.; Kampel, I.; Kaltenberger, F.; Pelikan, B. State of technology and design guidelines for the Archimedes screw turbine. In Proceedings of the Hydro 2012—Innovative Approaches to Global Challenges, Bilbao, Spain, 29–31 October 2012.
46. Rosly, C.; Jamaludin, U.; Azahari, N.; Nik Mutasim, M.; Oumer, A.; Rao, N.T. Parametric study on efficiency of archimedes screw turbine. *ARPN J. Eng. Appl. Sci.* **2016**, *11*, 10904–10908.
47. Lubitz William, D.; Lyons, M.; Simmons, S. Performance Model of Archimedes Screw Hydro Turbines with Variable Fill Level. *J. Hydraul. Eng.* **2014**, *140*, 04014050. [CrossRef]
48. Songin, K.J.; Lubitz, W.D. Measurement of fill level and effects of overflow in power-generating Archimedes screws. *J. Hydraul. Res.* **2019**, *57*, 635–646. [CrossRef]
49. Dellinger, G.; Terfous, A.; Garambois, P.-A.; Ghenaim, A. Experimental investigation and performance analysis of Archimedes screw generator. *J. Hydraul. Res.* **2016**, *54*, 197–209. [CrossRef]
50. Kozyn, A.; Lubitz, W.D. A power loss model for Archimedes screw generators. *Renew. Energy* **2017**, *108*, 260–273. [CrossRef]
51. Saroinsong, T.; Soenoko, R.; Wahyudi, S.; Sasongko, M.N. The effect of head inflow and turbine axis angle towards the three row bladed screw turbine efficiency. *Int. J. Appl. Eng. Res.* **2015**, *10*, 16977–16984.
52. Saroinsong, T.; Soenoko, R.; Wahyudi, S.; Sasongko, M.N. Performance of three-bladed Archimedes screw turbine. *ARPN J. Eng. Appl. Sci.* **2016**, *11*, 9491–9495.
53. Saroinsong, T.; Soenoko, R.; Wahyudi, S.; Sasongko, M.N. Effect of froude number on three-bladed archimedes screw turbine efficiency. *Int. J. Renew. Energy Res.* **2016**, *6*, 1153–1158.
54. Simmons, S.; Dellinger, G.; Lyons, M.; Terfous, A.; Ghenaim, A.; Lubitz William, D. Effects of Inclination Angle on Archimedes Screw Generator Power Production with Constant Head. *J. Hydraul. Eng.* **2021**, *147*, 04021001. [CrossRef]
55. Suraya, N.; Jamaludin, U.; Nik Mutasim, M. Investigation on the effect of drive train system for archimedes screw turbine. *ARPN J. Eng. Appl. Sci.* **2017**, *12*, 4809–4812.
56. DeChambeau, D. On her majesty's service. *Int. Water Power Dam Constr.* **2012**, *64*, 32–34.
57. Bauyon, J. Archimedes screw turbine as an energy conversion device for a run-of-river micro-hydropower plant. *J. Nucl. Energy Sci. Power Gener. Technol.* **2018**, 7.
58. Atkin, S. The 21st Century Archimedes Screw: New Materials and Manufacturing Techniques Enable the Turbine's Highest-Ever Measured Efficiency. 2021. Available online: https://www.energy.gov/eere/water/articles/21st-century-archimedes-screw-new-materials-and-manufacturing-techniques-enable (accessed on 1 October 2022).
59. Bloxham, G.J. Apparatus and Method for Forming a Screw Flight. U.S. Patent US9555457B2, 5 July 2012. Available online: https://patents.google.com/patent/US20140196515A1/en (accessed on 1 October 2022).
60. Walker, S.; Howell, R.; Hodgson, P.; Griffin, A. Tidal energy machines: A comparative life cycle assessment study. *Proc. Inst. Mech. Eng. Part M J. Eng. Marit. Environ.* **2013**, *229*, 124–140. [CrossRef]
61. Omodara, L.; Saavalainen, P.; Pitkäaho, S.; Pongrácz, E.; Keiski, R.L. Sustainability assessment of products-Case study of wind turbine generator types. *Environ. Impact Assess. Rev.* **2023**, *98*, 106943. [CrossRef]

62. Rueda-Bayona, J.G.; Cabello Eras, J.J.; Chaparro, T.R. Impacts generated by the materials used in offshore wind technology on Human Health, Natural Environment and Resources. *Energy* **2022**, *261*, 125223. [CrossRef]
63. Das, U.; Nandi, C. Life cycle assessment on onshore wind farm: An evaluation of wind generators in India. *Sustain. Energy Technol. Assess.* **2022**, *53*, 102647. [CrossRef]
64. Ozsahin, B.; Elginoz, N.; Germirli Babuna, F. Life cycle assessment of a wind farm in Turkey. *Environ. Sci. Pollut. Res.* **2022**, *29*, 71000–71013. [CrossRef]
65. Hindle, N.; Boersma, B. Archimedean Screw Apparatus. 2016. Available online: https://patentimages.storage.googleapis.com/cf/01/95/9b30ce59aebf2d/EP0161787A2.pdf (accessed on 1 October 2022).
66. Bizzarri, M.; Bartoň, M. Manufacturing of Screw Rotors Via 5-axis Double-Flank CNC Machining. *Comput.-Aided Des.* **2021**, *132*, 102960. [CrossRef]
67. Matejic, M.; Dragoi, M.V.; Blagojevic, M.; Filip, A.; Miletic, I. Progressive screw shaft manufacturing technology. *IOP Conf. Ser. Mater. Sci. Eng.* **2021**, *1009*, 012038. [CrossRef]
68. Swetha, R.; Siva Rama Krishna, L.; Hari Sai Kiran, B.; Ravinder Reddy, P.; Venkatesh, S. Comparative study on life cycle assessment of components produced by additive and conventional manufacturing process. *Mater. Today Proc.* **2022**, *62*, 4332–4340. [CrossRef]
69. Lapeyre, J.M. Mould and Process for Manufacturing Helical Shaped Items. U.S. Patent EP0161787A2, 9 April 1985.
70. Jung, I.D. Process and design optimization for powder injection molding of turbocharger vanes. *Met. Powder Rep.* **2021**, *76*, 26–29. [CrossRef]
71. Bianchi, M.F.; Gameros, A.A.; Axinte, D.A.; Lowth, S.; Cendrowicz, A.M.; Welch, S.T. Regional temperature control in ceramic injection moulding: An approach based on cooling rate optimisation. *J. Manuf. Process.* **2021**, *68*, 1767–1783. [CrossRef]
72. Upadhyayula, V.K.K.; Gadhamshetty, V.; Athanassiadis, D.; Tysklind, M.; Meng, F.; Pan, Q.; Cullen, J.M.; Yacout, D.M.M. Wind Turbine Blades Using Recycled Carbon Fibers: An Environmental Assessment. *Environ. Sci. Technol.* **2022**, *56*, 1267–1277. [CrossRef] [PubMed]
73. Shahbazi, M.; Jäger, H. Current Status in the Utilization of Biobased Polymers for 3D Printing Process: A Systematic Review of the Materials, Processes, and Challenges. *ACS Appl. Bio Mater.* **2021**, *4*, 325–369. [CrossRef] [PubMed]
74. Shashank, L.; Gokul, R.; Rajath, N.R.; Satwik Bhat, S. Theoretical analysis and fabrication of portable Archimedes screw micro hydro generator. *Int. J. Adv. Res. Sci. Eng. Technol.* **2021**, *8*, 17993–18002.
75. Sari, D.; Saputra, M.; Syofii, I.; Adanta, D. A Study of the Developing Archimedes Screw as a Turbine. *Int. J. Adv. Res.* **2021**, *87*, 151–160. [CrossRef]
76. Straalsund Jerry, L.; Harding Samuel, F.; Nuernbergk Dirk, M.; Rorres, C. Experimental Evaluation of Advanced Archimedes Hydrodynamic Screw Geometries. *J. Hydraul. Eng.* **2018**, *144*, 04018052. [CrossRef]
77. Lee, K.T.; Kim, E.-S.; Chu, W.-S.; Ahn, S.-H. Design and 3D printing of controllable-pitch archimedean screw for pico-hydropower generation. *J. Mech. Sci. Technol.* **2015**, *29*, 4851–4857. [CrossRef]
78. Olivera, A.F.; Chica, E.; Colorado, H.A. Evaluation of Recyclable Thermoplastics for the Manufacturing of Wind Turbines Blades H-Darrieus. In *Characterization of Minerals, Metals, and Materials 2022*; Springer: Cham, Switzerland, 2022; pp. 341–348.
79. Gomes, T.E.P.; Cadete, M.S.; Dias-de-Oliveira, J.; Neto, V. Controlling the properties of parts 3D printed from recycled thermoplastics: A review of current practices. *Polym. Degrad. Stab.* **2022**, *196*, 109850. [CrossRef]
80. Serra, A.; Malarco, M.; Musacchio, A.; Buia, G.; Bartocci, P.; Fantozzi, F. Comparing environmental impacts of additive manufacturing vs. Investment casting for the production of a shroud for gas turbine. In Proceedings of the ASME Turbo Expo, Virtual, 7–11 June 2021.
81. Torres-Carrillo, S.; Siller, H.R.; Vila, C.; López, C.; Rodríguez, C.A. Environmental analysis of selective laser melting in the manufacturing of aeronautical turbine blades. *J. Clean. Prod.* **2020**, *246*, 119068. [CrossRef]
82. Chang, J.; He, J.; Mao, M.; Zhou, W.; Lei, Q.; Li, X.; Li, D.; Chua, C.-K.; Zhao, X. Advanced Material Strategies for Next-Generation Additive Manufacturing. *Materials* **2018**, *11*, 166. [CrossRef]
83. Kankala, R.K.; Zhu, K.; Li, J.; Wang, C.-S.; Wang, S.-B.; Chen, A.-Z. Fabrication of arbitrary 3D components in Cardiac Surgery: From Macro-, Micro- to Nanoscale. *Biofabrication* **2017**, *9*, 032002. [CrossRef] [PubMed]
84. Sarraf, F.; Hadian, A.; Churakov, S.V.; Clemens, F. EVA-PVA binder system for polymer derived mullite made by material extrusion based additive manufacturing. *J. Eur. Ceram. Soc.* **2022**, *43*, 530–541. [CrossRef]
85. Spiller, S.; Berto, F.; Javad Razavi, S.M. Mechanical behavior of Material Extrusion Additive Manufactured components: An overview. *Procedia Struct. Integr.* **2022**, *41*, 158–174. [CrossRef]
86. Miclette, O.; Côté, R.; Demers, V.; Brailovski, V. Material extrusion additive manufacturing of low-viscosity metallic feedstocks: Performances of the plunger-based approach. *Addit. Manuf.* **2022**, *60*, 103252. [CrossRef]
87. Dezaki, M.L.; Serjouei, A.; Zolfagharian, A.; Fotouhi, M.; Moradi, M.; Ariffin, M.K.A.; Bodaghi, M. A review on additive/subtractive hybrid manufacturing of directed energy deposition (DED) process. *Adv. Powder Mater.* **2022**, *1*, 100054. [CrossRef]
88. Markus, D.; Lorin, A.; Thomas, N.; Sven, M. Identifying an opportunistic method in design for manufacturing: An experimental study on successful a on the manufacturability and manufacturing effort of design concepts. *Procedia CIRP* **2021**, *100*, 720–725. [CrossRef]

89. Tessarolo, A.; Luise, F.; Pieri, S.; Benedetti, A.; Bortolozzi, M.; De Martin, M. Design for Manufacturability of an Off-Shore Direct-Drive Wind Generator: An Insight into Additional Loss Prediction and Mitigation. *IEEE Trans. Ind. Appl.* **2017**, *53*, 4831–4842. [CrossRef]
90. Premkumar, V.; Krishnamurty, S.; Wileden, J.C.; Grosse, I.R. A semantic knowledge management system for laminated composites. *Adv. Eng. Inform.* **2014**, *28*, 91–101. [CrossRef]
91. Pietropaoli, M.; Ahlfeld, R.; Montomoli, F.; Ciani, A.; D'Ercole, M. Design for Additive Manufacturing: Internal Channel Optimization. *J. Eng. Gas Turbines Power* **2017**, *139*, 102101. [CrossRef]
92. Clemens, F.; Sarraf, F.; Borzì, A.; Neels, A.; Hadian, A. Material extrusion additive manufacturing of advanced ceramics: Towards the production of large components. *J. Eur. Ceram. Soc.* **2022**, *in press*. [CrossRef]
93. Adhikary, P.; Roy, P.; Mazumdar, A. Selection of hydro-turbine blade material-Application of Fuzzy Logic (MCDA). *Int. J. Eng. Res. Appl.* **2013**, *3*, 426–430.
94. Okokpujie, I.P.; Okonkwo, U.C.; Bolu, C.A.; Ohunakin, O.S.; Agboola, M.G.; Atayero, A.A. Implementation of multi-criteria decision method for selection of suitable material for development of horizontal wind turbine blade for sustainable energy generation. *Heliyon* **2020**, *6*, e03142. [CrossRef] [PubMed]
95. Kathwadia, A.; Parmar, K.; Acharya, G. Life Cycle Assessment of Turbine Blade. In Proceedings of the 3rd Afro-Asian International Conference on Science, Engineering & Technology, Gujarat, India, 27–28 March 2015.
96. Walker, S.R.J.; Thies, P.R. A life cycle assessment comparison of materials for a tidal stream turbine blade. *Appl. Energy* **2022**, *309*, 118353. [CrossRef]
97. Oliveira, P.; Martins, N.; Fontes, P.; Covas, D. Hydroenergy Harvesting Assessment: The Case Study of Alviela River. *Water* **2021**, *13*, 1764. [CrossRef]
98. Ceran, B.; Jurasz, J.; Wróblewski, R.; Guderski, A.; Złotecka, D.; Kaźmierczak, Ł. Impact of the Minimum Head on Low-Head Hydropower Plants Energy Production and Profitability. *Energies* **2020**, *13*, 6728. [CrossRef]
99. Musacchio, A.; Bartocci, P.; Serra, A.; Cencioni, L.; Colantoni, S.; Fantozzi, F. Decarbonizing materials sourcing and machining in the gas turbine sector, through a cost-carbon footprint nexus analysis. *J. Clean. Prod.* **2021**, *310*, 127392. [CrossRef]
100. Miklautsch, P.; Hoffelner, M.; Woschank, M. Harmonizing "Smart" Life Cycle Assessment in Manufacturing Companies: Literature Review and Preliminary Morphological Analysis. *IFAC-PapersOnLine* **2022**, *55*, 1483–1490. [CrossRef]
101. Ammar, M.; Haleem, A.; Javaid, M.; Walia, R.; Bahl, S. Improving material quality management and manufacturing organizations system through Industry 4.0 technologies. *Mater. Today Proc.* **2021**, *45*, 5089–5096. [CrossRef]
102. Paturi, U.M.R.; Cheruku, S.; Reddy, N.S. Artificial neural networks modelling for power coefficient of Archimedes screw turbine for hydropower applications. *J. Braz. Soc. Mech. Sci. Eng.* **2022**, *44*, 447. [CrossRef]
103. Kozyn, A.; Songin, K.; Gharabaghi, B.; Lubitz William, D. Predicting Archimedes Screw Generator Power Output Using Artificial Neural Networks. *J. Hydraul. Eng.* **2018**, *144*, 05018002. [CrossRef]
104. Lisicki, M.; Lubitz, W.; Taylor, G.W. Optimal design and operation of Archimedes screw turbines using Bayesian optimization. *Appl. Energy* **2016**, *183*, 1404–1417. [CrossRef]
105. YoosefDoost, A.; Lubitz, W.D. Archimedes Screw Design: An Analytical Model for Rapid Estimation of Archimedes Screw Geometry. *Energies* **2021**, *14*, 7812. [CrossRef]